30

Conducting Charge or Not

CHAPTER PREVIEW

Ceramics show the widest range of electrical properties of any class of material. At one extreme we have high-temperature superconductors, which have no resistance to an electrical current. At the other extreme we have electrical insulators. Ceramic superconductors have not yet fulfilled many of the expectations and predications for useful applications, whereas insulating ceramics are used for a number of critical applications such as packages for integrated circuits. Without the use of insulating ceramics the development of powerful personal computers would not have been so rapid. Between the two extremes are ceramics that behave very much like metals, and there are the semiconductors, which are all ceramics. Ceramics with metal-like conductivity are used as electrodes and in thick-film resistors. Semiconductors such as SiC are important for high-temperature electronics. In this chapter we will explain why ceramics show such a diverse range of electrical properties. The important concepts are related to our earlier discussion of bonding and energy bands.

In some ceramics the only species that can move in an applied electric field are the ions in the structure. Generally, the movement of ions is slow, but in a class of ceramics called fast ion conductors, they can move very rapidly. In cubic zirconia the diffusion of oxygen ions at high temperature is particularly fast, and this ceramic is used as the electrolyte in solid oxide fuel cells. Fuel cells are becoming a key part of a diverse energy plan for the twenty-first century.

We will begin by describing the conduction mechanisms in ceramics and looking at some specific applications. We will finish by describing one of the most fascinating developments in ceramics—high-temperature superconductors.

30.1 CERAMICS AS ELECTRICAL CONDUCTORS

Ceramics are usually thought of as electrical insulators and indeed a great many of them are. Since the first uses of electricity it has been necessary to have good electrical insulators to isolate current-carrying wires. The expansion of the electrical industry and, in particular, the use of the electric telegraph required enormous numbers of porcelain insulators for telegraph poles. From 1888 ceramics based on steatite began to be used for the same purpose. Today ceramics are still used to provide insulating supports in the power lines that criss-cross the country.

ELECTRIC TOWN

In 1881 Godalming became the first town in the world to have a public electricity supply.

The distinction between materials as electrical conductors and materials as insulators was made in the eighteenth century. Although historically the insulating properties of ceramics have often been one of their most important properties, many ceramics are actually very good electrical conductors and some are even superconductors. Ceramics show the broadest range of electrical properties of any of the classes of material. The values of electrical conductivity for ceramics vary over an enormous range—over 24 orders of magnitude!—as shown in Figure 30.1.

Table 30.1 lists the important parameters that are used in discussions of electrical conductivity. As we have done elsewhere in this book we will use SI units (unless there is a good reason for not doing so, such as the use of electron volts for band gap energies). If another system is widely used the appropriate conversion factor is given. Electrical conductivity is in general a tensor of the second rank. Fortunately, the electrical properties of materials can largely be understood by assuming that they are isotropic and σ is simply a scalar.

The conduction mechanisms in ceramics can be quite complex and may involve the movement of electrons,

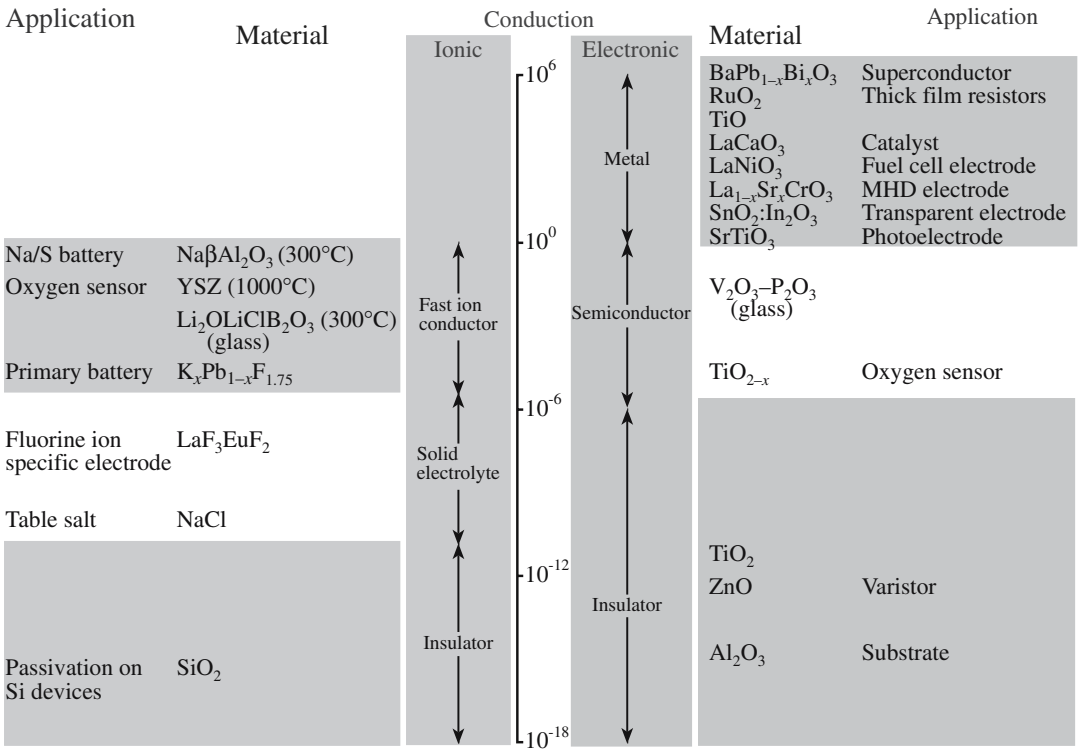

FIGURE 30.1 Range of conductivities of ceramics.

holes, and ions; in some cases they may be "mixed," with more than one type of charge carrier responsible for current flow. In the case of ceramic superconductors the current is carried by electron pairs (Cooper pairs). So this is really very different and is discussed separately.

In comparing values of σ and ρ it is useful to remember the simple relationship between them:

$$\sigma = \frac{1}{\rho} \tag{30.1}$$

TABLE 30.1 Terms and Units Used

Parameter	*Definition*	*Units/value*	*Conversion factor*
E_g	Band gap energy	eV	$1\,eV = 1.602 \times 10^{-19}$ J (eV is a much more convenient unit for E_g)
E_f	Fermi energy		
σ	Conductivity	S/m	$1\,S = 1\ \Omega^{-1}$
I	Current	A	
J	Current density	$C\,m^{-2}\,s^{-1}$	
v	Drift velocity	m/s	
ξ	Electric field strength	V/m	
μ	Mobility	$m^2\,V^{-1}\,s^{-1}$	Subscripts e and h will be used to represent electron and hole mobility, respectively; the units are the same in both cases
R	Resistance	Ω	
ρ	Resistivity	Ω·m	
V	Voltage	V	
q	Electron charge	1.602×10^{-19} C	Sometimes e
t	Transference number	Dimensionless	
K	Boltzmann constant	1.381×10^{-23} J/K	
T	Temperature	K or °C	
T_c	Critical temperature for superconductivity	K	0 K = –273°C

30.2 CONDUCTION MECHANISMS IN CERAMICS

Electrical conductivity is given by

$$\sigma = nq\mu \tag{30.2}$$

The importance of Eq. 30.2 is that it applies to all materials and it shows that the two factors affecting σ are

- Number of charge carriers, n
- Their mobility, μ

When we consider the effect of variables such as composition, structure, and temperature on σ we are concerned with their effect on n and μ.

If more than one type of charge carrier is contributing to σ then we can define a partial conductivity for each. For example, if σ were due to the movement of electrons and cations with a charge Z, then for electrons

$$\sigma_e = \mu_e\ (n_e q) \tag{30.3}$$

and for cations

$$\sigma_+ = \mu_+\ (n_+ Zq) \tag{30.4}$$

The total is

$$\sigma_{tot} = \sigma_e + \sigma_+ \tag{30.5}$$

If a ceramic is an electron conductor, i.e., $t_e = 1$, then to determine n we need to know E_g. We usually consider the three situations shown in Figure 30.2, where the band gap is either zero, narrow, or wide.

TABLE 30.2 Transference Numbers of Cations, t_+, Anions, t_-, and Electrons or Holes, $t_{e,h}$ in Several Materials

Ceramic	*T (°C)*	t_+	t_-	$t_{e,h}$
NaCl	400	1.00	0.00	
	600	0.95	0.05	
KCl	435	0.96	0.04	
	600	0.88	0.12	
KCl + 0.02% $CaCl_2$	430	0.99	0.01	
	600	0.99	0.01	
AgCl	20–350	1.00		
AgBr	20–300	1.00		
BaF_2	500		1.00	
PbF_2	200		1.00	
CuCl	20			1.00
	366	1.00		
ZrO_2 + 7% CaO	>700		1.00	$<10^{-4}$
$Na_2O{\cdot}11Al_2O_3$	<800	1.00 (Na^+)		$<10^{-6}$
FeO	800	10^{-4}		1.00
ZrO_2 + 18% CeO_2	1500		0.52	0.48
ZrO_2 + 50% CeO_2	1500		0.15	0.85
$Na_2O{\cdot}CaO{\cdot}SiO_2$ glass		1.00 (Na^+)		
15% $(FeO{\cdot}Fe_2O_3){\cdot}CaO{\cdot}SiO_2{\cdot}Al_2O_3$ glass	1500	0.1 (Ca^{2+})		0.9

TRANSFERENCE NUMBER

The transference or transport number is the fraction of σ_{tot} contributed by each charge carrier.

For electrons: $t_e = \sigma_e/\sigma_{tot}$
For cations: $t_+ = \sigma_+/\sigma_{tot}$

Table 30.2 lists examples of t.

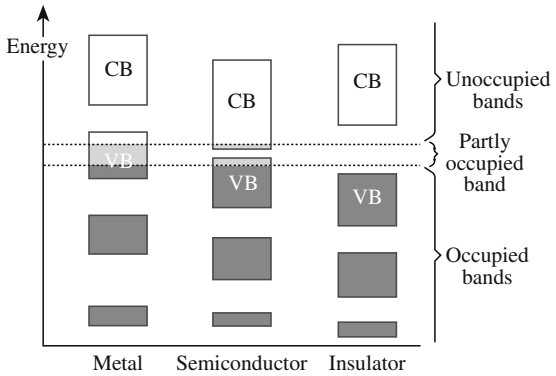

FIGURE 30.2 Schematic of electron energy bands in solids. The valence band (VB) and conduction band (CB) are indicated.

The real band structure of a material is actually a complex three-dimensional shape. Even so these simple representations can be used to illustrate many of the important electronic properties of materials. When E_g is zero, as in the case of most metals, there are free electrons present at any temperature above 0 K. The total number of free electrons is equal to the number of valence electrons per atom multiplied by the number of atoms in the metal.

E_g in a metal is not zero, but it is very small. For example, if we have a metal crystal consisting of 10^{23} atoms and the width of the energy band is 1 eV then the separation between the energy levels would be only 10^{-23} eV (1.6×10^{-42} J). This would be the minimum amount of energy required to excite an electron into a vacant level.

A narrow band gap is usually defined as being in the range of 0.02 to about 2.5 eV. When E_g is toward the lowest end of this range there is a significant fraction of electrons in the conduction band. Materials with a narrow band gap are usually referred to as semiconductors.

- Silicon: $E_g = 1.12$ eV
- Gallium arsenide: $E_g = 1.42$ eV

Both Si and GaAs are ceramics.

TABLE 30.3 Band Gap Energies for Various Ceramics

Material	E_g *(eV)*	*Material*	E_g *(eV)*	*Material*	E_g *(eV)*
		Halides			
AgBr	2.80	BaF_2	8.85	CaF_2	12.00
KBr	0.18	KCl	7.00	LiF	12.00
MgF_2	11.00	MnF_2	15.50	NaCl	7.30
NaF	6.70	SrF_2	9.50	TlBr	2.50
		Oxides			
Al_2O_3 (sapphire)	8.80	CdO	2.10	Ga_2O_3	4.60
MgO (periclase)	7.7	SiO_2 (fused silica)	8.30	UO_2	5.20
CoO	4.0	CrO_3	2.0	Cr_2O_3	3.3
CuO	1.4	Cu_2O	2.1	FeO	2.4
Fe_2O_3	3.1	MnO	3.6	MoO_3	3.0
Nb_2O_5	3.9	NiO	4.2	Ta_2O_5	4.2
TiO_2 (rutile)	3.0–3.4	V_2O_5	2.2	WO_3	2.6
Y_2O_3	5.5	ZnO	3.2	$BaTiO_3$	2.8–3.2
$KNbO_3$	3.3	$LiNbO_3$	3.8	$LiTaO_3$	3.8
$MgTiO_3$	3.7	$NaTaO_3$	3.8	$SrTiO_3$	3.4
$SrZrO_3$	5.4	$Y_3Fe_5O_{12}$	3.0		
		Carbides and Nitrides			
AlN	6.2	BN	4.8	C (diamond)	5.33
SiC (α)	2.60–3.20a				
		Chalcogenides			
PbTe	0.275	PbS (galena)	0.350	PbSe	0.400
CdTe	1,450	CdSe	1.850	CdS	2.420
ZnSe	2.600	ZnS	3.600		

Materials with a wide band gap (>2.5 eV) are considered to be electrical insulators because the probability of an electron being in the conduction band at room temperature is extremely small. However, the probability is not zero and so we should think of these materials as wide-band-gap semiconductors. SiC ($E_g = 2.6$–3.0) is an example of a wide-band-gap semiconductor and is used in sensors in aircraft and fuel cells that can operate in hostile environments at temperatures up to 600°C where conventional silicon-based electronics cannot function.

Band gap energies for a number of ceramics are listed in Table 30.3.

30.3 NUMBER OF CONDUCTION ELECTRONS

This section follows directly from Section 4.8. The number of electrons in the conduction band, n_i, is

$$n_i = \int_{E_c}^{E_{top}} N_c(E) f(E) dE \tag{30.6}$$

- $N_c(E)\,dE$ is the density of states in the conduction band and represents the number of energy levels over which the electrons can be distributed (i.e., the number of allowed energy states).
- $P(E)$ is the Fermi–Dirac function giving the probability of an electron being in the conduction band.

$$f(E) = \left\{ \frac{1}{\left[1 + \exp\left(\frac{E - E_f}{kT}\right)\right]} \right\} \tag{30.7}$$

The evaluation of n_i is quite straightforward if we make the following assumptions:

1. $E - E_f \gg kT$. This is often the case since at room temperature $kT \sim 0.025$ eV and $E - E_f$ is usually >5 eV. We can now omit the +1 in Eq. 30.7. [We are in effect replacing Fermi–Dirac statistics by Boltzmann statistics.]
2. The excited electrons occupy states near the bottom of the conduction band. Under these conditions they behave as free particles for which the state distribution function is known.
3. The upper limit of the integration in Eq. 30.6 is taken as ∞ since the probability of occupancy of a state by an electron rapidly approaches zero as the energy increases through the band.

Under these assumptions we can write

$$n_i = N_c \exp\left(-\frac{E_c - E_F}{kT}\right) \tag{30.8}$$

E_F lies midway between E_C and E_V in an intrinsic material (i.e., one that has few impurities) and since $N_C \sim 10^{25}\,m^{-3}$ we can simplify Eq. 30.8 as

$$n_i = N_c \exp\left(-\frac{E_g}{2kT}\right) \sim 10^{25} \exp\left(-\frac{E_g}{2kT}\right) \tag{30.9}$$

The important things to remember from this series of equations are that

- n depends on E_g and T.
- As we increase T we increase n.

30.4 ELECTRON MOBILITY

As electrons move through a solid under the influence of ξ they experience a number of collisions (in a process called scattering) that decreases μ. There are three scattering mechanisms:

- *Phonon*. This is the major factor affecting μ (of both electrons and holes). A phonon is the quantum unit of lattice vibrational energy as described later in Chapter 34. The higher the temperature the greater the vibrational amplitude of the atoms in the lattice and the greater the number of phonons. As a result, scattering increases and μ decreases with increasing temperature.

$$\mu \propto T^{-m} \tag{30.10}$$

- *Electron–electron*. At room temperature the mean distance between electron–electron collisions is about 10 times that of electron–phonon collisions so electron–phonon scattering is dominant.
- *Polaron*. This mechanism occurs only in ionic crystals and involves the interaction between the electron and the ions in the crystal. The electron can cause local distortion of the lattice known as a polaron as illustrated in Figure 30.3. When the interaction is sufficiently strong (small polaron) the electron may be trapped at a particular lattice site, reducing μ and decreasing σ.

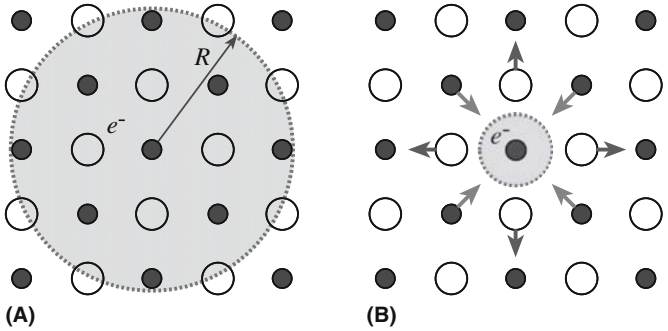

FIGURE 30.3 Illustration of (a) a large polaron of radius R, formed in a metal oxide MO and (b) a small polaron, showing the distortion of the lattice around an electron trapped at a metal.

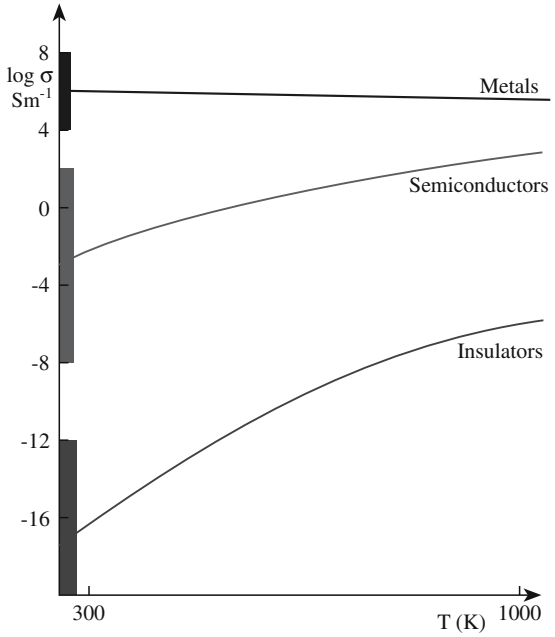

FIGURE 30.4 Conductivity variations with temperature for the different classes of electrical conductor. The shading indicates the range of values at room temperature.

30.5 EFFECT OF TEMPERATURE

For a material where $E_g = 0$, i.e., one in which n does not vary significantly with T, σ decreases with increasing temperature because of the decrease in μ:

$$\sigma \propto \frac{n}{T^m} \tag{30.11}$$

For materials where $E_g > 0$ (i.e., materials that we would classify as semiconductors or insulators), σ rises with T because of the temperature dependence of n as shown by Eq. 30.9:

$$\sigma \propto \exp\left(-\frac{E}{2kT}\right) \tag{30.12}$$

Figure 30.4 shows the typical T dependence of σ for the three broad classes of electrical behavior.

Because it is possible to make practical use of the variation in σ or ρ with T it is often beneficial to classify materials based on this variation. (From a practical point of view we usually consider changes in ρ rather than changes in σ.) The temperature dependence of resistivity may be expressed by an empirical equation

$$\rho_2 = \rho_1[1 + \alpha_R(T_2 - T_1)] \tag{30.13}$$

where ρ_1 is the resistivity at T_1 and ρ_2 is the resistivity at T_2. The parameter α_R is known as the temperature coefficient of resistivity or TCR. For materials where $E_g = 0$ the TCR is typically positive. These materials are called positive temperature coefficient (PTC) materials. Most materials that show semiconducting or insulating properties are negative temperature coefficient (NTC) materials. Some ceramics, for example $BaTiO_3$, that do have energy band gaps are actually PTC materials. This type of behavior has nothing to do with conduction across the band gap but is actually a grain boundary (GB) effect.

30.6 CERAMICS WITH METAL-LIKE CONDUCTIVITY

The general electrical characteristics of metals are

- $\sigma \geq 10^4$ S/m
- $t_e = 1$
- $n = 10^{22}$–10^{23} cm^{-3}
- $d\sigma/dT$ is small and negative.

Remember that Ω^{-1} (ohm^{-1}) is S (siemens). Some ceramics, for example TiO and VO, show metallic-like electronic conductivity where the conduction is due to the movement of free electrons. To explain this behavior we will consider the example of TiO.

TiO has a structure based on rocksalt with vacancies in both the metal and oxygen sublattices. One-sixth of the titaniums and one-sixth of the oxygens are missing as illustrated in Figure 30.5. The 2p orbitals from the oxygen atoms form a filled valence band. The bands formed by the 4s and 4p orbitals on the Ti are at a much higher energy. The metal d orbitals form a band below that of the metal s and p orbitals as illustrated in Figure 30.6.

TRANSITION METALS
Transition metals have partially filled d orbitals.

ELECTRON CONFIGURATIONS

Ti	$1s^2 2s^2 2p^6 3s^2 3p^6 3d^2 4s^2$
Ti^{2+}	$1s^2 2s^2 2p^6 3s^2 3p^6 3d^2$
Ti^{4+}	$1s^2 2s^2 2p^6 3s^2 3p^6$

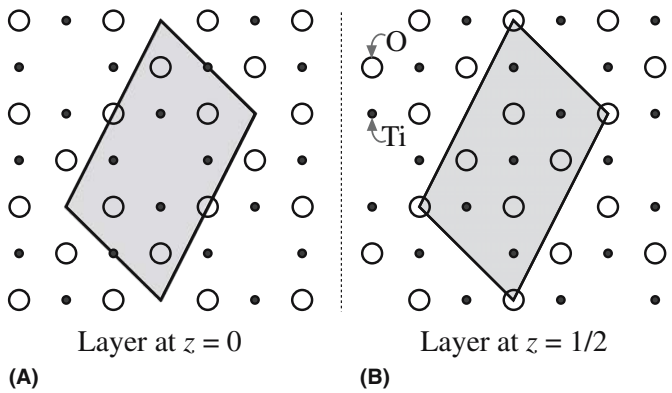

FIGURE 30.5 The structure of TiO. (a) The (100) plane. (b) The (200) plane. Both show the absence of alternate ions along <110> directions. The resultant superlattice has a monoclinic unit cell as indicated by the shaded region.

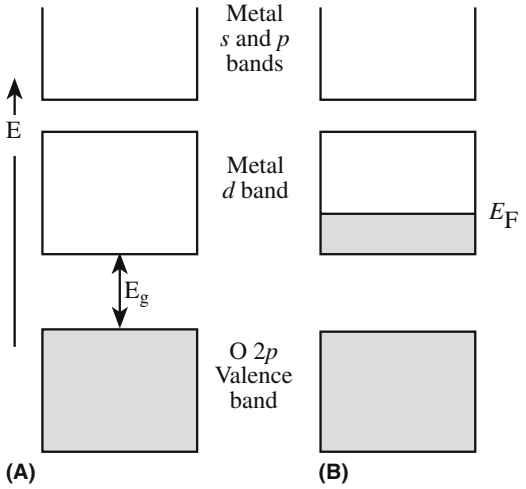

FIGURE 30.6 Energy bands of a transition metal oxide: (a) d band empty; (b) metallic oxide with d band partially filled.

The divalent titanium ion, Ti^{2+}, in TiO has two 3d electrons and so the metal d band shown in Figure 30.6 is partially filled. It is this partially filled band, which you will notice resembles the energy level diagram for a metal shown in Figure 30.2, that leads to metallic conductivity in TiO. Looking at Figure 30.6 it is easy to see why titanium dioxide, TiO_2, is an insulator. In the formation of the Ti^{4+} ion, both the two 4s electrons and the two 3d electrons are given up to form oxygen ions. So the 3d band (the conduction band in the solid) is empty at $T = 0$ K. The band gap, E_g, in TiO_2 is 3 eV. This is a relatively small E_g for an insulator and indicates some covalent character in the Ti–O bond.

So why aren't MnO, CoO, and NiO, which are also monoxides of the first row transition metals and have the rocksalt structure, metallic-like conductors?

To answer this question we need to consider the interaction between the d orbitals and the formation of the d band in metal oxides. In the rocksalt structure the d_{xy}, d_{yz}, and d_{xz} orbitals (collectively known as the t_{2g} orbitals) on adjacent metal atoms overlap. The extent of the overlap is less than it would be in the pure metal because in the oxides the metal atoms are not nearest neighbors. Consequently the d bands are narrower than they would be for the metal. (We are referring to the widths of the bands themselves and not the size of the band gap.) As we go across the first row transition elements (from Ti to Ni) there is an increase in nuclear charge and a corresponding

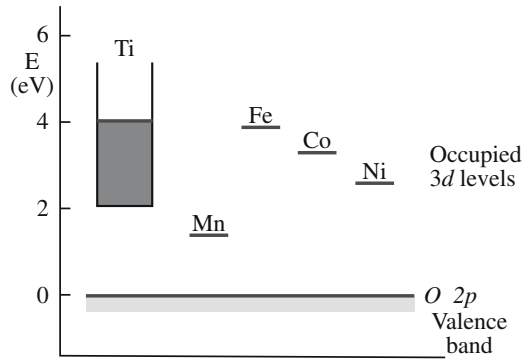

FIGURE 30.7 Electronic energy levels of some 3d monoxides, deduced from spectroscopic measurements. The energy zero has been taken as the top of the oxygen 2p valence band.

contraction in the size of the d orbitals. As the d orbitals become smaller the extent of overlap decreases and the 3d band becomes narrower, eventually forming a localized state as illustrated in Figure 30.7.

Some oxides of the second and third row transition elements also exhibit metallic-like properties, for example, ReO_2 and ReO_3. In these compounds the metal electron energy levels of interest are the 5d, rather than the 3d as in the case of the first row transition metals.

Figure 30.8 shows the σ versus temperature behavior for several oxides. For some of the oxides we have already mentioned, e.g., ReO_3, TiO, CrO_2, and ReO_2, $d\sigma/dT$ is small and negative, just like it is for most metals.

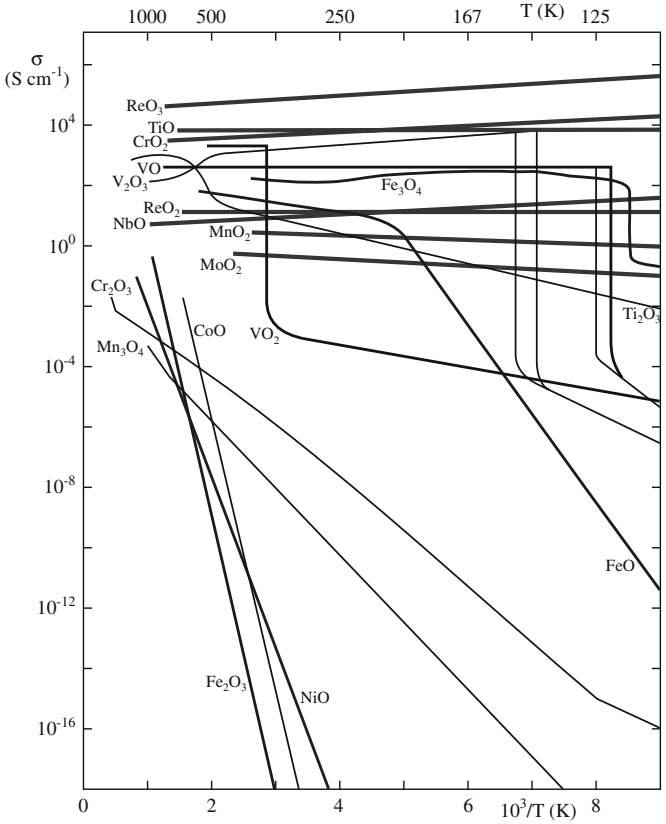

FIGURE 30.8 Temperature dependence of the electrical conductivity of several electronically conducting oxides.

30.7 APPLICATIONS FOR HIGH-σ CERAMICS

There are many applications for ceramics that have metal-like conductivity. We will look at two examples:

- Resistors
- Electrodes

Resistors

The requirements for most resistors are that they are

- Ohmic
- Small TCR

Components with R in the range 10^3–$10^8\,\Omega$ are the major requirements of the electronic industry. These are fabricated from electronically conducting ceramics with σ in the range 10^5–10^6 S/m. Resistance is not an intrinsic property of a material. It is influenced by the specimen configuration, i.e., its thickness and length. The relationship between R and σ is

$$R = \frac{l}{\sigma A} \tag{30.14}$$

where A is the cross-sectional area of the specimen perpendicular to the direction of the current flow and l is the distance between the two points at which the voltage is measured. To make a 10^5-Ω resistor of length 10 cm from a material with $\sigma = 10^6$ S/m would require a cross-sectional area of $10^{-12}\,m^2$. Using a strip with a $1\,\mu m^2$ cross section would be possible, but it is not usually economically feasible. There are two methods that are used to make high-resistance components using high-σ ceramics:

1. Increase the aspect ratio (length to width) of the conductive layer by patterning
2. Mix the conductive phase with a highly resistive one

Thin-film resistors usually make use of the first approach. For example, thin films (~10 nm thick) of indium tin oxide (ITO) are deposited onto glass, or sometimes steatite, substrates by sputtering or chemical vapor deposition (CVD). After deposition the films are patterned to achieve a large aspect ratio. If the substrate is in the form of a rod a spiral groove is cut into the film.

Thick-film resistors are made by diluting a conductive oxide with an electrical insulator such as glass. (The practical aspects of thick-film processing were described in

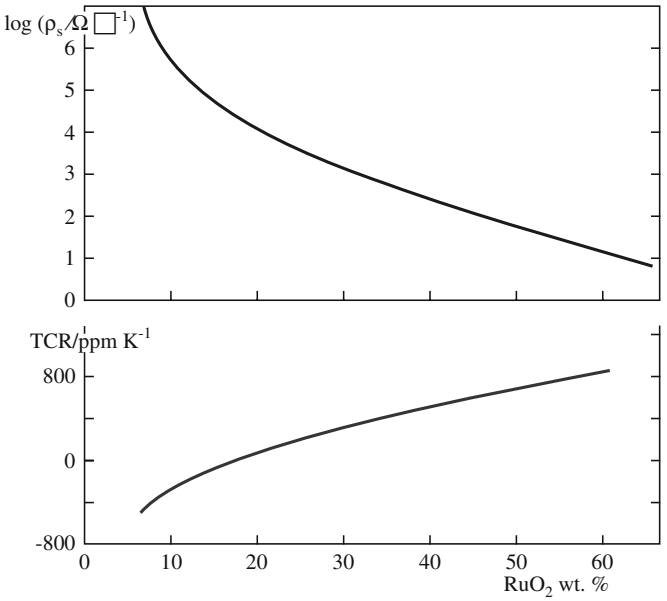

FIGURE 30.9 Electrical characteristics of RuO_2 thick-film resistors.

Chapter 27.) Ruthenium dioxide (RuO_2) and mixed metal oxides containing ruthenium, such as $Bi_2Ru_2O_7$, are widely used as the conducting component. These oxides have σ in the range of 10^5–10^6 S/m. The glass is usually a lead borosilicate of composition typically (in wt%) 52PbO–35SiO_2–10B_2O_3–3Al_2O_3. The final thickness of the resistor after processing is in the range of 10–15 μm. The resistors normally have high resistivities and negative TCRs for low concentrations of the conductive component and low resistivities and positive TCRs for high concentrations as shown in Figure 30.9. This behavior is the result of a combination of the positive TCR of the conductive particles and the negative TCR of the regions between them.

The distribution of the conductive particles and the contact between them also determines the resistance of the deposited film. Final resistance values are obtained either by sand blasting, where the thickness of the film is reduced, or by laser trimming, to increase the effective length of the resistor. These procedures would be performed after the resistor has been fired, but before the application of the protective glaze coating.

Electrodes

High-σ ceramics are used as electrodes in a number of applications:

- Fuel cells
- Humidity sensors
- Displays

The question we need to ask ourselves again is: What is special about ceramics?

Temperature Stability. $LaCrO_3$ was developed in the 1960s for electrodes in magnetohydrodynamic (MHD) generators where the electrode had to withstand temperatures up to 2000°C and the corrosive potassium atmosphere in the generator. $LaCrO_3$ has a melting temperature of 2500°C and σ = 100 S/m at 1400°C. MHD generators are now of little interest, but $LaCrO_3$ has been used as an electrode in solid oxide fuel cells. $LaCrO_3$ has the perovskite structure that we described in Chapter 7.

Porous. In humidity and gas sensors the electrode must be electrically conductive, produce a porous coating (to allow the vapors to reach the sensor), and be stable in the sensing environment. RuO_2 is used as an electrode in humidity sensors. One example of the sensing element is a solid solution of TiO_2 in $MgCr_2O_4$. This type of sensor is used in microwave ovens where it detects the rapid rise in humidity corresponding to the onset of cooking. There is a fall in ρ when the ceramic is exposed to humid atmospheres, the result of dissociation of water molecules:

$$2H_2O = H_3O^+ + OH^- \qquad (30.15)$$

Several other materials have been developed for humidity sensors and the electrical responses of three different ones are shown in Figure 30.10.

Transparent. For applications in which a transparent electrode is required metals are completely unsuitable. Metals, because of their very small E_g, can absorb all wavelengths of visible light and are, as a result, opaque in the visible part of the electromagnetic spectrum. Only metal layers <1 μm will be transparent. A ceramic used as a transparent electrode is indium tin oxide (ITO). A typical electrode composition is 90In_2O_3–10SnO_2. Transparent electrodes are important for many electrooptic devices,

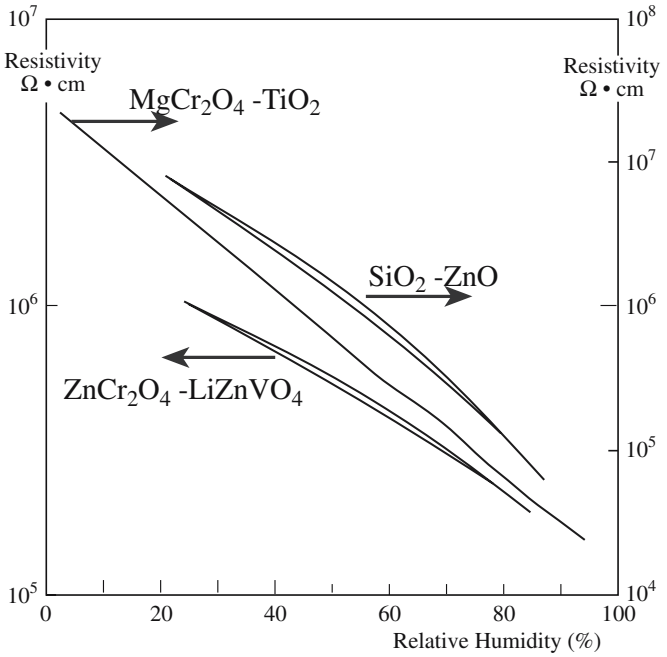

FIGURE 30.10 Electrical response of three ceramic humidity sensors at room temperature and 1 kHz.

liquid crystal displays (LCDs), light-emitting diodes (LEDs), and solar cells.

30.8 SEMICONDUCTING CERAMICS

Semiconductors have a small E_g as shown in Figure 30.2. In semiconductors σ is proportional to n and μ (for both electrons and holes). In general, there are three ways free electrons and holes may be generated in ceramics:

- Excitation across the band gap (*intrinsic* semiconductors)
- Introduction of impurities/dopants (*extrinsic* semiconductors)
- Departures from stoichiometry (*nonstoichiometric* semiconductors)

Most oxide semiconductors are either doped to create extrinsic defects or are annealed under conditions in which they become nonstoichiometric.

Intrinsic Semiconductors

For every electron that is excited into the conduction band, a hole is produced in the valence band.

The number of electrons in the conduction band is

$$n = N_c \exp\left(-\frac{E_g}{2kT}\right) \tag{30.16}$$

Similarly, the number of holes in the valence band is

$$p = N_v \exp\left(-\frac{E_g}{2kT}\right) \tag{30.17}$$

The densities of states are given by

$$N_c = 2\left(\frac{2\pi m_e^* kT}{h^2}\right)^{3/2} \tag{30.18}$$

and

$$N_v = 2\left(\frac{2\pi m_h^* kT}{h^2}\right)^{3/2} \tag{30.19}$$

where m_e^* and m_h^* are the effective masses of the electrons and holes, respectively. For many ceramics m_e^* and m_h^* are not known and we make the (often incorrect) assumption that $m_e = m_e^* = m_h^*$, where m_e is the rest mass of the electron.

If we use the subscript i to denote intrinsic carrier concentrations, we can write

$$n_i = p_i \tag{30.20}$$

and

$$np = n_i p_i = n_i^2 \tag{30.21}$$

Therefore

$$n_i = (N_c N_v)^{1/2} \exp\left(-\frac{E_g}{2kT}\right) \tag{30.22}$$

If $N_c = N_v$ then

$$n_i = N_c \exp\left(-\frac{E_g}{2kT}\right) \tag{30.23}$$

The intrinsic conductivity is given by

$$\sigma_i = q n_i (\mu_e + \mu_h) \tag{30.24}$$

MOBILITIES OF ELECTRONS AND HOLES
In ceramics these depend upon their interaction with the lattice. Typical values are very small ($\leq 0.1\,cm^2\,V^{-1}\,s^{-1}$): orders of magnitude lower than in Si and GaAs.

Equation 30.24 is similar to Eq. 30.2, but we are now considering μ_e and μ_h.

The intrinsic conductivity of many pure oxide semiconductors is generally very low because of their large E_g compared to Si and GaAs. To illustrate this point we will compare the room temperature conductivities of Cu_2O, a semiconducting oxide E_g = 2.1 eV, and GaAs, a III–V semiconductor E_g = 1.4 eV.

The largest applications for semiconductors use extrinsic material. The entire electronic materials industry is built around doped silicon. However, there are applications that require intrinsic semiconductors. One such application is X-ray detectors used on transmission electron microscopes (TEMs) and scanning electron microscopes (SEMs) for chemical analysis. Unfortunately it is essentially impossible to produce pure silicon. Even electronic grade silicon contains small amounts of boron (a p-type dopant). To create "intrinsic" material a dopant is added that produces an excess of electrons that combine with the holes formed by the residual boron. The process involves diffusing lithium atoms into the semiconductor. Ionization of the lithium produces electrons that recombine with the holes. It is possible to produce germanium crystals with much higher purity, and intrinsic Ge detectors are used on some TEMs.

Extrinsic and Nonstoichiometric Semiconductors

An extrinsic semiconductor contains impurities that are present either accidentally or, as is most often the case, that have been intentionally added. The effect of these impurities on the energy band diagram is that they introduce additional energy levels into the band gap as illustrated in Figure 30.11. These new energy levels are often close to the band edges.

If the impurity level is just above the valence band the impurity is an "acceptor" because it can accept electrons leaving holes in the valence band. If the impurity can supply electrons into the conduction band it is a "donor" and the level is located just below the bottom of the conduction band. If the impurity acts as an electron donor the semiconductor is known as an n-type semiconductor because the electrons (or negatively charged species) are the majority charge carriers. If the impurity acts as an electron acceptor then the semiconductor is known as a p-type semiconductor because holes (or positively charged species) act as the majority charge carriers.

At low temperatures the number of charge carriers is determined by the donor and acceptor ionization energies. At sufficiently high temperatures full ionization of the impurities is achieved and the carrier densities become independent of temperature. This region is called the "exhaustion" or "saturation" region. At even higher temperatures the thermal energy is enough to excite electrons across the energy band gap and the material behaves like an intrinsic semiconductor. These three regions are shown in Figure 30.12.

Nonstoichiometric semiconductors are very similar to extrinsic semiconductors, and can really be con-

WORKED EXAMPLE

1. *Calculate N_c and N_v* (Eqs. 30.18 and 30.19) (*density of states*):

   Cu_2O: we will assume $m_e^* = m_h^* = 9.11 \times 10^{-32}$ kg
   $\Rightarrow N_c = N_v = 2.49 \times 10^{19}\,cm^{-3}$

   GaAs: $m_e^* = 0.067m_e = 6.10 \times 10^{-32}$ kg,
   $m_h^* = 0.48m_e = 4.37 \times 10^{-31}$ kg $\Rightarrow$
   $N_c = 4.31 \times 10^{17}\,cm^{-3}$ and
   $N_v = 8.26 \times 10^{18}\,cm^{-3}$

2. *Calculate n_i* (Eq. 30.23):

   Cu_2O: $n_i = 45.11\,cm^{-3}$; GaAs: $n_i = 2.85 \times 10^6\,cm^{-3}$

3. *Calculate* σ (Eq. 30.24):

The last parameters we need before we can calculate n_i are μ_e and μ_h. In ionic solids these values are often not well known, but are several orders of magnitude lower than for the covalent semiconductors.

Cu_2O: $\mu_e = 0.2\,cm^2\,V^{-1}\,s^{-1}$ and $\mu_h = 0.1\,cm^2\,V^{-1}\,s^{-1}$.

(Reasonable estimates.) For GaAs see Table 30.4.

Cu_2O: $\sigma = 2.17 \times 10^{-18}$ S/cm;
GaAs $\sigma = 5 \times 10^{-9}$ S/cm

These are room temperature values for "pure" materials.

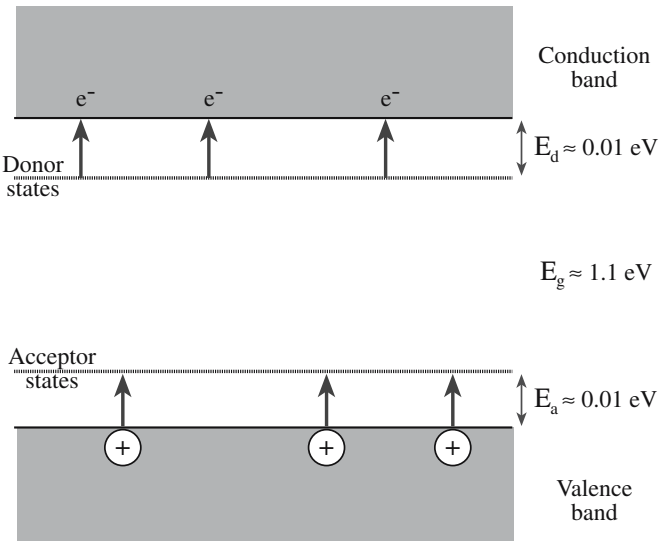

FIGURE 30.11 Effect of doping on band structure.

TABLE 30.4 Mobilities of Various Semiconductors

Semiconductor	*Electron mobility* ($m^2\,V^{-1}\,s^{-1}$)	*Hole mobility* ($m^2\,V^{-1}\,s^{-1}$)
α-SiC	0.04	~0.02
Si	0.15	0.049
Ge	0.39	0.18
GaAs	0.85	0.30
InAs	3.30	0.02
InSb	8.00	0.17
Diamond	0.18	0.12
PbS	0.06	0.02
GaSb	0.30	0.065
CdS	0.04	—
CdSe	0.065	—
CdTe	0.12	0.005
GaP	0.015	0.012
AlN	—	0.001
PbSe	0.09	0.07
PbTe	0.17	0.093
AgCl	0.005	—
SnO_2	0.016	—
$SrTiO_3$	0.0006	—
Fe_2O_3	10^{-5}	—
TiO_2	2×10^{-5}	—
Fe_3O_4	—	10^{-5}
$CoFe_2O_4$	10^{-8}	10^{-12}
FeO, MnO, CoO, NiO		~10^{-5}

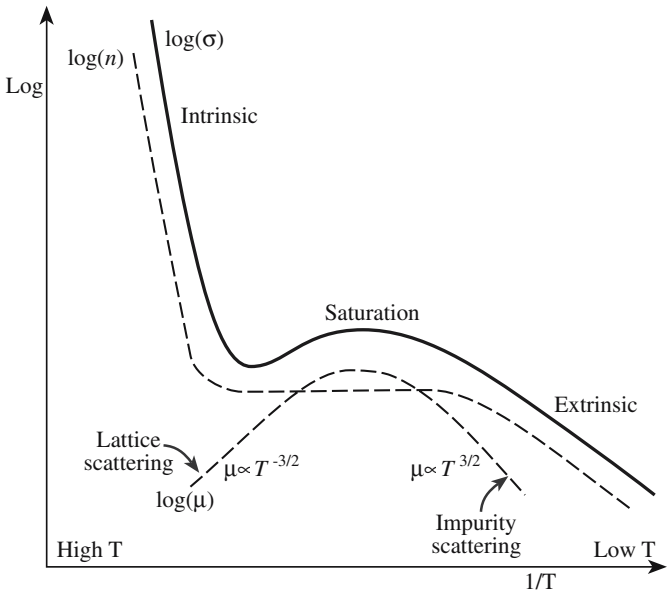

FIGURE 30.12 Temperature dependence of σ for an extrinsic semiconductor. The dashed lines show the individual contributions of *n* and μ to σ.

sidered together. The main difference is that the electronic defects rather than being due to impurity atoms are the result of changes in the stoichiometry of the crystal. We still use the designations n- and p-type to describe the majority charge carrier and the defect adds levels into the band gap that lead to increased levels of conductivity, particularly at room temperature and below.

30.9 EXAMPLES OF EXTRINSIC SEMICONDUCTORS

Zinc Oxide: An n-Type Semiconductor

In Section 11.7 we described the result of heating ZnO in Zn vapor. The excess Zn atoms occupy interstitial sites. One electron is produced for every Zn interstitial as shown using Kröger–Vink notation:

$$\mathrm{Zn(g)} \rightarrow \mathrm{Zn_i^{\cdot}} + \mathrm{e'} \qquad (11.13)$$

The requirement of electroneutrality means that the concentration of interstitials is equal to the concentration of electrons:

$$[\mathrm{Zn_i}] = [\mathrm{e'}] = K p_{\mathrm{Zn}}{}^{1/2} \qquad (11.14)$$

Because σ depends on the number of charge carriers it will be proportional to the zinc vapor pressure:

$$\sigma \propto p_{\mathrm{Zn}}{}^{1/2} \qquad (30.25)$$

The oxygen dependence can be considered in a similar way and gives

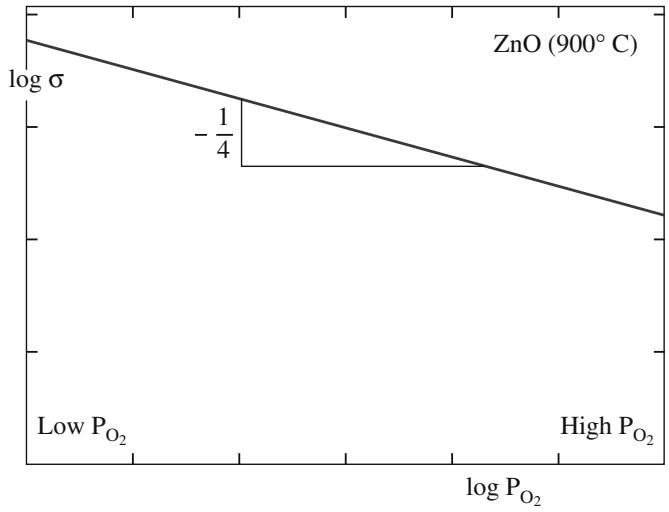

FIGURE 30.13 Effect of oxygen pressure on the electrical conductivity of ZnO.

$$[\mathrm{Zn_i}] = [\mathrm{e'}] = K p\mathrm{O_2}^{-1/4} \qquad (30.26)$$

Now σ will be vary with the oxygen partial pressure as shown in the log–log plot in Figure 30.13:

$$\sigma \propto p\mathrm{O_2}^{-1/4} \qquad (30.27)$$

Figure 30.14 shows the energy band diagram for $\mathrm{Zn_{1+x}O}$ illustrating the positions of the donor levels. E_1 and E_2 are

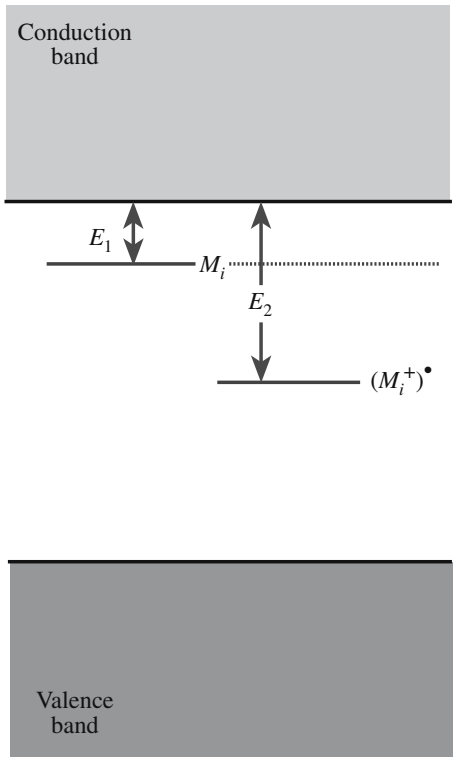

FIGURE 30.14 Schematic representation of the energy levels in $\mathrm{Zn_{1+x}O}$.

the first and second ionization energies for Zn. At low temperatures the electrons would not be excited into the conduction band and would be localized at the donor level. As the temperature rises, the fraction of electrons in the conduction band increases. At a sufficiently high temperature all the impurity atoms will be ionized.

Copper Oxide: A p-Type Semiconductor

If we start with stoichiometric Cu_2O and remove a copper atom to form a copper vacancy, the charge balance requires formation of a hole as shown using Kröger–Vink notation:

$$(Cu_{Cu})^X \rightarrow Cu(g) + (V_{Cu})' + h^{\cdot} \qquad (30.28)$$

For a possible second ionization state

$$(V_{Cu})' \rightarrow (V_{Cu})'' + h^{\cdot} \qquad (30.29)$$

The above processes are shown on an energy band diagram in Figure 30.15.

We can also consider that a hole forms by the production of vacancies on the cation sublattice when pO_2 is increased. The overall reaction can be represented as

$$1/2O_2\ (g) \rightarrow (O_O)^X + 2(V_{Cu})' + 2h^{\cdot} \qquad (30.30)$$

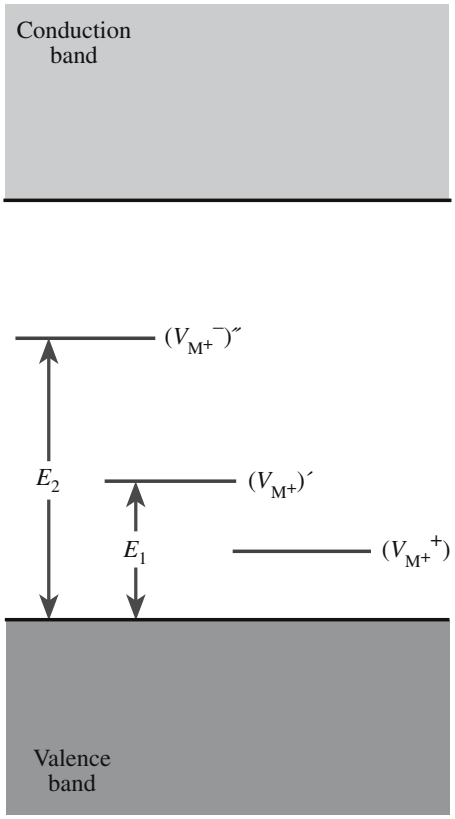

FIGURE 30.15 Schematic representation of energy levels in a deficit semiconductor such as $Cu_{2-x}O$.

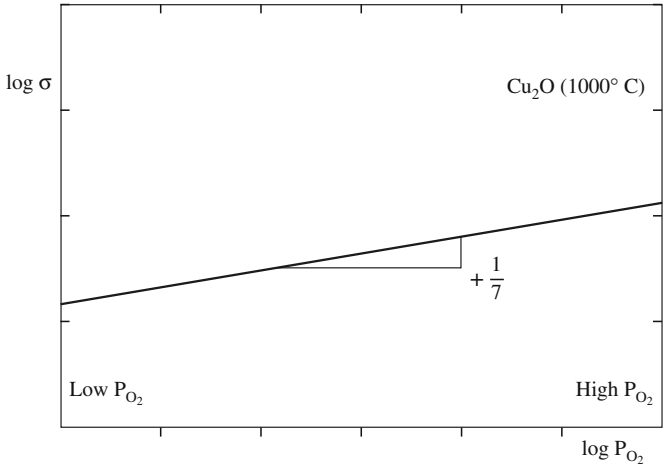

FIGURE 30.16 Conductivity of Cu_2O as a function of pO_2.

(You will recognize Eq. 30.30 as being similar to Eq. 11.8.)

Using the same approach that we used for ZnO we can obtain a relationship between pO_2 and σ:

$$\sigma \propto [h^{\cdot}] = K(T)^{1/4} pO_2^{1/8} \qquad (30.31)$$

Experimentally, as illustrated in Figure 30.16, σ is found to be proportional to $pO_2^{1/7}$, which is in reasonable agreement with Eq. 30.31.

There are many examples of impurity semiconductors and a partial list is given in Table 30.5.

30.10 VARISTORS

A varistor is used in an electric circuit as protection against large voltage pulses, i.e., a surge protector. Such devices are particularly important in protecting microelectronic devices. ZnO is the most widely used and important material for varistors.

Under normal operating conditions a small current will flow through the varistor. If the voltage rises above some threshold value (for example, the result of a voltage

TABLE 30.5 Partial List of Impurity Semiconductors

n-Type					
TiO_2	Nb_2O_5	CdS	Cs_2Se	$BaTiO_3$	Hg_2S
V_2O_5	MoO_2	CdSe	BaO	$PbCrO_4$	ZnF_2
U_3O_8	CdO	SnO_2	Ta_2O_5	Fe_3O_4	
ZnO	Ag_2S	Cs_2S	WO_3		
p-Type					
Ag_2O	CoO	Cu_2O	SnS	Bi_2Te_3	MoO_2
Cr_2O_3	SnO	Cu_2S	Sb_2S_3	Hg_2O	MnO
NiO	Pr_2O_3	CuI			

spike in the power supply) a large current will flow through the varistor to ground before it can damage the circuit. To operate in this way a varistor must have a highly nonlinear *I–V* relationship, as shown in Figure 30.17.

- At low applied voltages the varistor behaves in an ohmic manner, i.e., there is a linear *I–V* relationship.
- When the applied voltage reaches a threshold value known as the breakdown voltage a large current flows, following a power law:

$$I \propto V^{\alpha} \tag{30.32}$$

The exponent α is used as a figure of merit for the varistor and can be as high as 70 for ZnO, although values in the range 25–45 are more typical. For SiC α ~ 5.

A significant difference between a varistor and a diode is that varistors can be used in both ac and dc circuits. Compare the plot shown in Figure 30.17 with what would be seen for a Zener diode.

The microstructure of a ZnO varistor is the key to its operation. Grains of about 15–20 μm in diameter are separated by a Bi-rich intergranular film (IGF) that varies in thickness from 1 nm to 1 μm, as illustrated in Figure 14.38. Varistor action is a result of a depletion region formed on either side of the IGF. To explain varistor behavior we use an approach very similar to that used to describe Schottky barriers in metal–semiconductor junctions.

Figure 30.18a shows an energy level diagram for two ZnO grains separated by an IGF. The bismuth that segregates to the GB results in the formation of acceptor levels. The way that the bismuth dopants produce these sites is not well understood, but possibly they stabilize acceptor defects such as Zn vacancies at the GB. At equilibrium the Fermi levels on each side of the boundary must line up, as shown in Figure 30.18b. This requirement is necessary because at equilibrium the probability of occupation of any quantum level must be independent of position. When this occurs, the conduction and valence bands bend, resulting in an energy barrier (height $e\phi$) at the GB. Conduction band electrons must surmount this energy barrier for conduction to occur. When a potential is applied across the varistor the size of the energy barrier is reduced. Conduction is provided by thermal activation of electrons across the barrier (at low fields) or tunneling (high fields). At the breakdown voltage the energy barrier is zero and a massive increase in electrical conduction occurs.

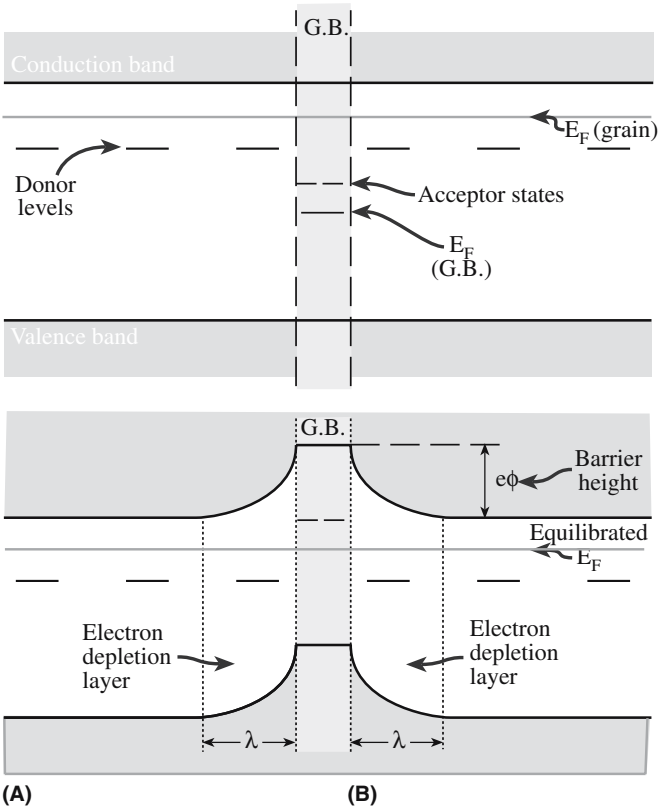

FIGURE 30.18 Proposed band diagram for two semiconducting ZnO grains separated by an IGF: (a) showing the location of acceptor sites in the IGF; (b) at equilibrium. Application of a potential decreases the barrier height.

Varistor breakdown is reversible and if the applied voltage is decreased below the breakdown value the varistor will return to ohmic behavior. The breakdown voltage is typically in the range of tens to hundreds of volts.

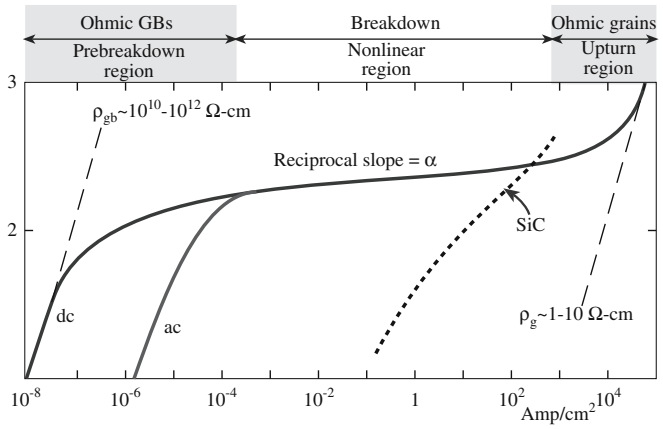

FIGURE 30.17 Typical *I–V* characteristic for a ZnO varistor.

- Single-crystal silicon diodes (avalanche or Zener) are used only for low-voltage applications.
- ZnO varistors are used for both low- and high-voltage applications.

30.11 THERMISTORS

Thermally sensitive resistors (thermistors) have high TCRs produced by one of the following mechanisms:

1. Excitation across the band gap—intrinsic semiconductor behavior resulting in an exponential decrease in ρ over a wide temperature range (NTC).

2. A structural phase transformation causing a change from semiconducting behavior to metallic conduction, which causes a large decrease in ρ over a small temperature range (NTC).

3. A change in the conductivity of the GB, which produces a large increase in ρ over a small temperature range (PTC).

In semiconductors such as SiC where NTC behavior is expected ρ varies with T according to

$$\rho(T) = \rho_\infty \exp(B/T) \tag{30.33}$$

ρ_∞ is approximately independent of temperature and B is a constant related to the energy required to excite the electrons into the conduction band. By differentiation we can obtain an expression for α:

$$\alpha_R = d\rho/\rho dT = -B/T^2 \tag{30.34}$$

α_R is usually expressed either as a percentage change in resistivity, e.g., $-3\%\,K^{-1}$, or in terms of ppm changes per degree change in temperature, e.g., ppm/°C. Table 30.6 shows the properties of thermistors based on Mn_3O_4 with partial replacement of the Mn by Ni, Co, and Cu.

NTC materials are used in many applications to either sense temperature or to respond to changes in temperature. One application is temperature sensors to measure the temperature of the cooling water in an automobile engine.

The behavior of PTC materials is very different from NTC materials. Commercial PTC devices rely on the changes associated with the ferroelectric Curie temperature (θ_c). Typical PTC behavior is shown in Figure 30.19. In regions AB and CD the material is showing NTC behavior. But at the Curie temperature (θ_c) there is a large positive change in ρ.

Polycrystalline lanthanum-doped $BaTiO_3$ (BLT) is one example of a PTC material. The effect is associated with GBs and is not observed in single crystals. At the GB there is a potential barrier (ϕ) preventing electron movement from one grain to an adjacent one (very similar to that caused by the IGF in ZnO). The GB resistance, R_{gb} is

$$R_{gb} \propto \exp(\phi/kT) \tag{30.35}$$

TABLE 30.6 Properties of Thermistor Compositions Based on Mn_3O_4 at 25°C

Composition (cat.%)						
Mn	*Co*	*Ni*	*Cu*	$\rho_{25}/\Omega\cdot m$	*B/K*	$\alpha_R/\%K^{-1}$
56	8	16	20	10^{-1}	2580	−2.9
65	9	19	7	1	2000	−2.2
70	10	20		10	3600	−4.0
85		15		10^2	4250	−4.7
94		6		10^3	4600	−5.1

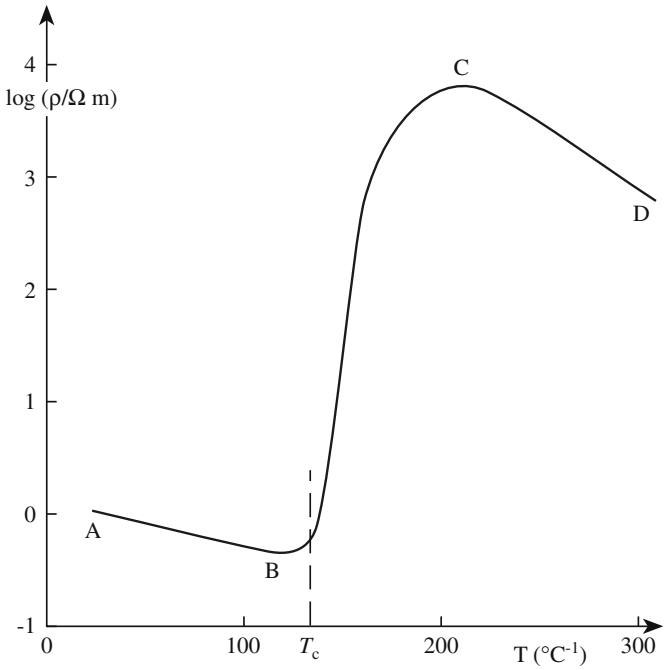

FIGURE 30.19 Typical characteristics of a PTC thermistor material.

Above θ_c

$$R_{gb} \propto \exp\left[N\left(1 - \frac{T_{cw}}{T}\right)\right] \tag{30.36}$$

where N is a temperature-independent constant for the particular material and includes specific details about the electronic structure of the grain boundary and T_{cw} is the Curie–Weiss temperature (~θ_c).

30.12 WIDE-BAND-GAP SEMICONDUCTORS

Wide-band-gap semiconductors refer to materials that have a band gap between about 2 and 5 eV. At present one of the most interesting wide-band-gap semiconductors is SiC, which has an E_g from 2.4 to 5.1 eV. These materials are important because they can be used at much higher temperatures than Si or GaAs because the thermal generation of electron-hole pairs is much lower. SiC exists in a number of different polytypes each having different properties as shown in Tables 30.7 and 30.8.

TABLE 30.7 Summary of Band Structures for SiC Polytypes

	3C	*6H*	*4H*	*2H*
Direct band gap (eV)	5.14	4.4	4.6	4.46
Indirect band gap (eV)				
Experimental	2.39	3.0	3.26	3.35
Theory	2.4	2.4	2.8	3.35

TABLE 30.8 Summary of Properties for n-Type SiC ($N_D = 6 \times 10^{16}$ cm^{-3}) at Room Temperature

Polytype	Electron mobility ($cm^2 V^{-1} s^{-1}$)	E_D (meV)	$m^*_{\parallel}/m_e$	$m^*_{\perp}/m_e$
4H	700	33	0.19	0.21
15R	500	47	0.27	0.25
6H	330	95	1.39	0.35

30.13 ION CONDUCTION

Ion movement can make a major contribution to σ, particularly if the material has a large E_g. Conductivity resulting from ion migration is important in several ceramics. It is also the major conduction mechanism in ionic salts such as the halides.

When we describe the mobility of ions we often use the absolute mobility, B:

$$B = \frac{v}{F} = \frac{v}{zeE} \tag{30.37}$$

where v is the drift velocity and F is the applied force (which in this case is the electrical potential, i.e., $F = Zq\xi$, where Z is the charge on the ion.)

B is related to μ:

$$\mu = ZqB \tag{30.38}$$

Substituting Eq. 30.38 into Eq. 30.2 gives

$$\sigma = nZq^2B \tag{30.39}$$

The absolute mobility, and hence σ, is directly related to the diffusion coefficient, D, through the Nernst–Einstein equation:

$$D = kTB \tag{30.40}$$

The diffusion coefficient is given by an Arrhenius equation, which means that there is an activation energy that must be overcome for the ions to move through the material as illustrated in Figure 30.20. We can then give σ in terms of D, which is what we did in Section 11.15:

$$\sigma = \frac{ne^2D}{kT} \tag{11.53}$$

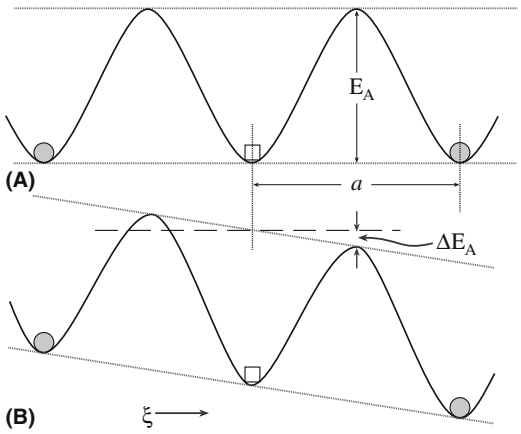

FIGURE 30.20 Potential energy barrier to ion movement. (a) In the absence of an applied field and (b) with an applied field. E_A is the activation energy and a the jump distance between ion sites.

The following factors contribute to ionic mobility:

- *Size.* It is easier to move a small ion than a large one.
- *Charge.* A highly charged ion will polarize, and be polarized by ions of opposite charge as it moves past them. This will increase E_A.
- *Lattice geometry.* Some structures contain channels that facilitate the ion movement. A large number of vacant sites can help.

30.14 FAST ION CONDUCTORS

Materials that show exceptionally high ionic conductivity are referred to as "fast ion" conductors or "superionic" conductors. The conductivities are comparable to those of electrolyte solutions, but are still low compared with metal-like electron conductivity. There are two important types of fast ion conductor:

1. The β-aluminas: nonstoichiometric aluminates, for example
   - $Na_2O \cdot 11Al_2O_3$ (β-alumina)
   - $Na_2O \cdot 8Al_2O_3$ (β′-alumina)
   - $Na_2O \cdot 5Al_2O_3$ (β″-alumina)

They all have a layer structure, as illustrated earlier in Figure 7.12, that is composed of spinel blocks of close-packed O^{2-} ions with Al^{3+} in tetrahedral and octahedral interstices. Planes containing Na^+ and O^{2-} ions separate the spinel blocks. It is within these planes that the mobility of the Na^+ ions is high. The conductivity is highly anisotropic; it is high within the Na^+-containing planes and negligible in the perpendicular direction.

2. Cubic stabilized zirconia stabilized usually with either CaO or Y_2O_3.

These materials have oxygen ion transport numbers very close to 1.0. To understand how they are able to conduct large oxygen ions it is necessary to consider their defect structure. The correct composition of an oxide with the fluorite structure oxide would be MO_2. The addition of CaO to ZrO_2, for example, drops the metal-to-oxygen ratio below 2.0, and the formula of the oxide becomes $Ca_xZr_{1-x}O_{2-x}$. As we showed in Section 11.7, the Ca^{2+} ions substitute for Zr^{4+} ions and we have compensating oxygen vacancies. For each substitutional Ca^{2+}, we must create one anion vacancy. The result of this enormous defect population is to greatly increase the diffusion coefficient for oxygen to the extent that this material becomes a very fast oxygen-ion conductor.

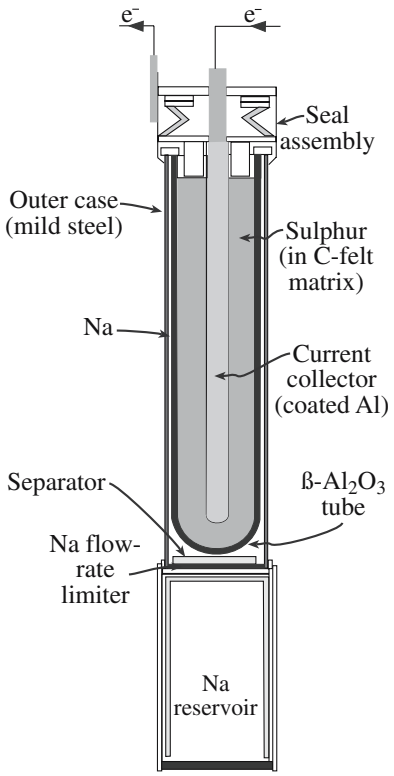

FIGURE 30.21 Schematic of a "central sulfur" cell. Typically, the electrolyte tube is some 300 mm long and 30 mm in diameter.

TABLE 30.9 Efficiency of Various Batteries

Type	*Efficiency (Wh/kg)*
Nickel–cadmium (Ni–Cd)	7–50
Nickel–metal hydride (Ni–H)	20–100
Sodium–sulfur	75–200

Stable ceramics that have completely ionic conductivity can be used as solid-state electrolytes. Two examples are the Na–S battery and the solid oxide fuel cell.

OTHER USES OF CERAMICS IN BATTERIES

Hg battery—HgO is the cathode.

Ni–Cd battery—hydrated NiO ($NiOOH \cdot H_2O$) is the cathode.

Li battery—MnO_2 is the cathode.

30.15 BATTERIES

A battery operates on the principle of a Galvanic cell; a chemical reaction is used to produce electricity. The materials that are involved in the reaction form the electrodes and the reaction takes place by the passage of ions through an electrolyte. The formation of ions during the chemical reaction involves the transfer of electrons to or from the electrodes. In a galvanic cell these are not allowed to pass through the electrolyte but must travel around an external circuit, driven by a potential difference created between the electrodes. It is the electron movement through the external circuit that can be used to do work.

β-Alumina is used as an electrolyte in high-energy-density Na–S batteries. The concept of a battery based on the reaction of Na and S was first proposed in 1967 as an alternative to the conventional lead-acid battery. The Na and S are separated by a membrane of β-alumina, usually in the form of a closed-end thin-walled tube as shown in Figure 30.21. It is often convenient to place the S inside the β-alumina tube since the ceramic has far superior corrosion resistance to that of the mild steel outer casing. On connection to the external circuit the Na gives up electrons forming Na^+ ions. These diffuse through the β-alumina to react with the S to produce the sulfide according to the reaction

$$2Na\ (l) + 5S\ (l) \rightarrow Na_2S_5\ (l) \qquad (30.41)$$

The reverse reaction occurs on recharging. The cell runs at about 300°C with both Na and S in the liquid state. The cell reaction is extremely energetic, and the heat required to maintain the cell at its operating temperature is readily supplied by the cell reaction itself.

Despite being used by the Ford Motor Company in a series of test vehicles the disadvantages of the Na–S battery, not least of all its cost (~$50,000 each), have limited its adoption for electric vehicle applications.

A different application proposed for Na–S batteries is for spacecraft. Since electrical power systems make up a major part of a spacecraft's weight and batteries are typically the largest component of the power system, it is critical to improve the efficiency of spacecraft batteries.

Battery efficiency is measured in terms of specific energy, or watt-hours of energy output per kilogram of battery weight (Wh/kg), and values for several batteries are given in Table 30.9. In 1996 an Na–S battery was flight tested during a space shuttle mission. Although cost is not as much of an issue with spacecraft as it is with automobiles, there are still technological challenges in using Na–S batteries. One of these challenges is producing a suitable casing. Steel containers, even with protective coatings, can easily be dented or scratched, leading to corrosion and rapid failure.

30.16 FUEL CELLS

A fuel cell is another example of a galvanic cell and supplies electrical energy in the same way as a battery. The essential difference between the two types of cell is that the electrodes of a fuel cell do not deteriorate chemically. Therefore, if a fuel cell is fed a constant supply of fuel it

TABLE 30.10 Fuel Cells and Their Applications

Fuel cell	*Electrolyte*	*Anode fuel*	*Cathode gas*	*Operating T(°C)*	*Applications*
Alkaline fuel cell (AFC)	KOH solution	H_2	O_2	60–90	Spacecraft, submarines
Proton exchange membrane fuel cell (PEMFC)	Proton conductive polymer membrane	H_2	O_2 (in air)	60–90	Transportation vehicles, stationary power plants, cogeneration plants, portable power supplies
Direct methanol fuel cell (DMFC)	Proton conductive polymer membrane	Methanol	O_2 (in air)	90–120	Transportation vehicles, stationary power plants, cogeneration plants, portable power supplies
Phosphoric acid fuel cell (PAFC)	Phosphoric acid	H_2	O_2 (in air)	200	Stationary power plants, cogeneration plants
Molten carbonate fuel cell (MCFC)	Molten alkaline carbonate	H_2, CH_4, or coal gas	O_2 (in air)	650	Stationary power plants, cogeneration plants
Solid oxide fuel cell (SOFC)	Ceramic solid electrolyte	H_2, natural gas, coal gas	O_2 (in air)	800–1000	Stationary power plants, cogeneration plants

will supply continuous electrical energy. The fuel is hydrogen or a hydrogen-rich source (e.g., methanol or formic acid).

The first practical fuel cell was developed in the 1950s at Cambridge University in the UK. The cell used Ni electrodes and an alkaline electrolyte. Pratt and Whitney further modified the alkaline fuel cell as it was called in the 1960s for NASA's Apollo program. The cells were used to provide on board electrical power and drinking water for the astronauts. The alkaline fuel cell proved successful, but it was an order of magnitude too expensive for terrestrial applications and demanded pure hydrogen and oxygen to operate.

Table 30.10 lists the different types of fuel cell that are being investigated together with some of their potential applications. Fuel cells are one of the leading research topics at the present time with the goal of reducing the dependence on fossil fuels and associated problems of global warming.

There are two types of fuel cell that use ceramics:

- Molten carbonate fuel cell (MCFC)
- Solid-oxide fuel cell (SOFC)

The main difference between the two types is in the electrolyte. The MCFC uses a molten carbonate immobilized in a porous $LiAlO_2$ matrix. The SOFC uses a ceramic membrane of cubic stabilized zirconia. An illustration of the operation of a SOFC is shown in Figure 30.22.

The cell reactions are

$$\text{Cathode:} \quad O_2 + 4e^- \rightarrow 2O^{2-}$$
$$\text{Anode:} \quad 2H_2 + 2O^{2-} \rightarrow 2H_2O + 4e^-$$
$$\text{Overall reaction:} \quad O_2 + 2H_2 \rightarrow 2H_2O$$

A single fuel cell supplies a dc voltage of <1 V. If larger voltages are required the cells must be stacked together in series. Commercially voltages up to ~200 V can be attained. The current produced is proportional to the area over which the reaction occurs. The best fuel cells at present provide a maximum current density of $0.5–2\ A/cm^2$.

MCFCs and SOFCs can be made by assembling individual plate cells into stacks, just like the design of the original voltaic pile. For SOFCs producing 5–200 kW ceramic plates from 150 mm to 300 mm square are required. This requirement presents a problem because it is difficult to produce large thin flat dense plates of ceramics. Siemens-Westinghouse developed an alternative tubular design; it is straightforward to extrude long tubes (see Section 23.9). The disadvantage of the tube design

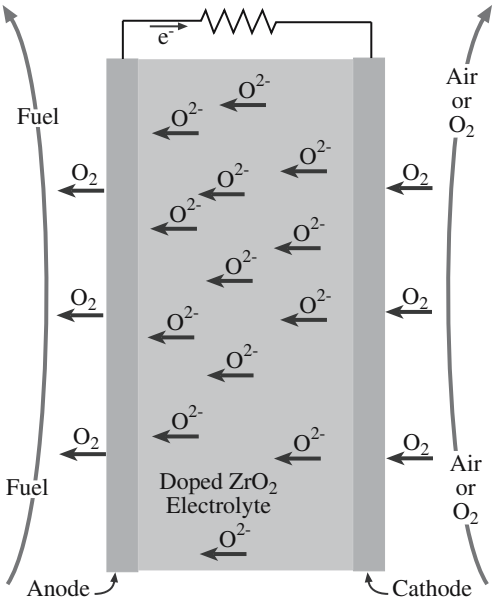

FIGURE 30.22 Simple representation of an SOFC using cubic zirconia.

is that it has high thermal inertia and a long warming time.

Fuel cells offer significant advantages over many other power sources. They are

- Silent
- Low maintenance
- Efficient (they are not limited to the Carnot efficiency—i.e., the maximum theoretical efficiency that can be obtained from an engine employing combustion)
- Nonpolluting (the product is distilled water)

These advantages are the reasons for the continued research efforts. However, we still do not know whether fuel cell technology can be made commercially viable (at the present time it is not).

A principle similar to that used in the SOFC can be applied to oxygen sensors for applications including monitoring of automobile exhaust emissions to increase engine efficiency and reduce emissions. Figure 11.17 can be compared to Figure 30.22 to see the similarities. Oxygen control is also important in several metallurgical processes such as gas carburizing and the bright annealing of stainless steel.

30.17 CERAMIC INSULATORS

More typically we think of ceramics as being good electrical insulators and there are many ceramics that have $\rho > 10^{14}\,\Omega\cdot$cm. Examples of common ceramic insulators include

- Aluminum oxide (Al_2O_3)
- Mullite ($3Al_2O_3 \cdot 2SiO_2$)
- Forsterite ($2MgO \cdot SiO_2$)
- Beryllium oxide (BeO)
- Aluminum nitride (AlN)

In an electrical insulator there is a wide energy gap between the bottom of the conduction band and the top of the valence band. Figure 30.23 shows the energy band diagram for MgO. The valence band is formed by the 2p energy levels of oxygen (O^{2-} ions) and the conduction band is formed from the empty 3s orbitals of the Mg^{2+} ions. The energy band gap is ~8 eV and the concentration of thermally excited electrons in the conduction band of MgO is low right up to its melting point, 2800°C. MgO is therefore an excellent high temperature insulator.

Very wide energy band gaps (>6 eV) are associated with compounds that have high fractions of ionic character in their bonding. Ions have a stable noble gas electron configuration. To excite an electron from the valence band to the conduction band involves making the electron configuration of the ions different from those of the noble gases. This process is energetically unfavorable.

In general, compounds with wide band gaps have

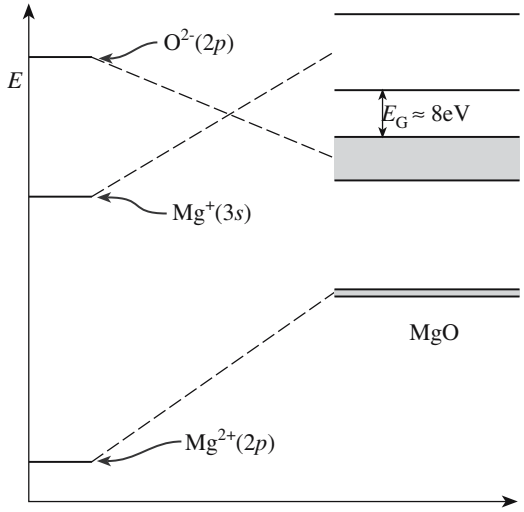

FIGURE 30.23 Energy band diagram for MgO.

- Predominantly ionic bonding
- Consist of atoms (ions) of low Z

Some ceramics having large values of E_g are listed in Table 30.3. No entirely satisfactory relationship has been established between the ionic character of the bond and the atom size on E_g. In a homologous series of oxides, such as the oxides of the alkaline-earth metals, E_g increases with increasing ionic potential, ϕ, of the cation as shown in Figure 30.24.

In a series of isoelectronic compounds (i.e., compounds with an identical total number of electrons) E_g increases

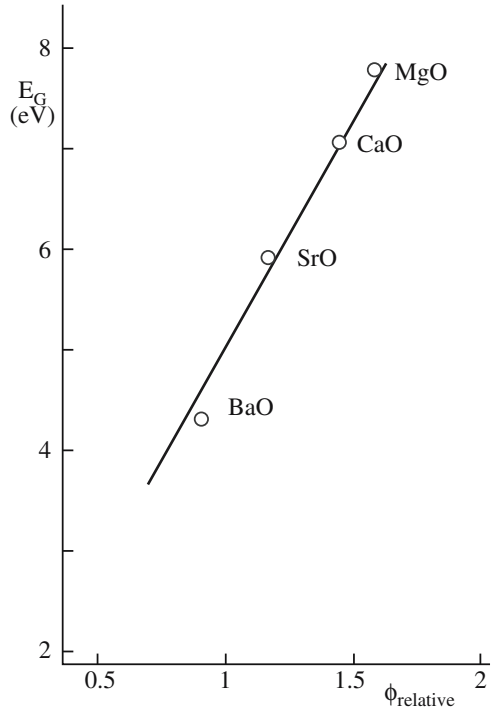

FIGURE 30.24 Effect of bond ionicity on E_g for metal oxides MO ($\phi = Z/r$).

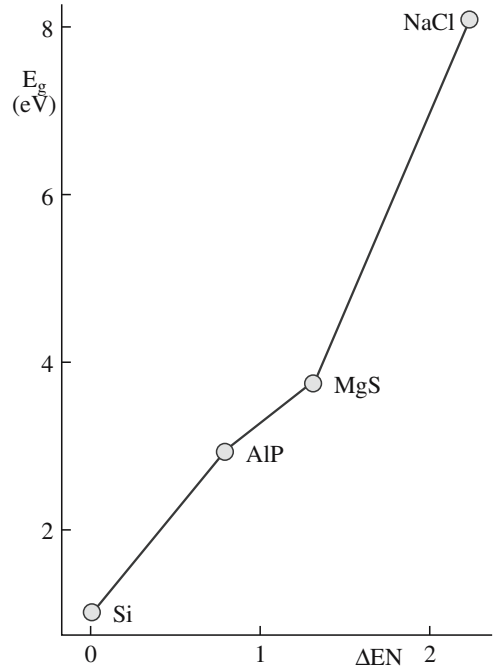

FIGURE 30.25 Correlation of E_g and electronegativity difference (ΔEN).

with the increasing ionic character of the interatomic bond as shown in Figure 30.25. Understanding this relationship is quite straightforward. As the fraction of covalent character in a bond increases the electrons in that bond are more equally shared and hence electron transfer becomes easier.

The presence of point defects in the lattice can be viewed as being donor or acceptor species in the same way that we considered defects in semiconductor crystals. Figure 30.26 shows another version of an energy band diagram for MgO, this time with the estimated defect energy levels included. If the crystal contains oxygen vacancies (i.e., it has been reduced) these can become ionized:

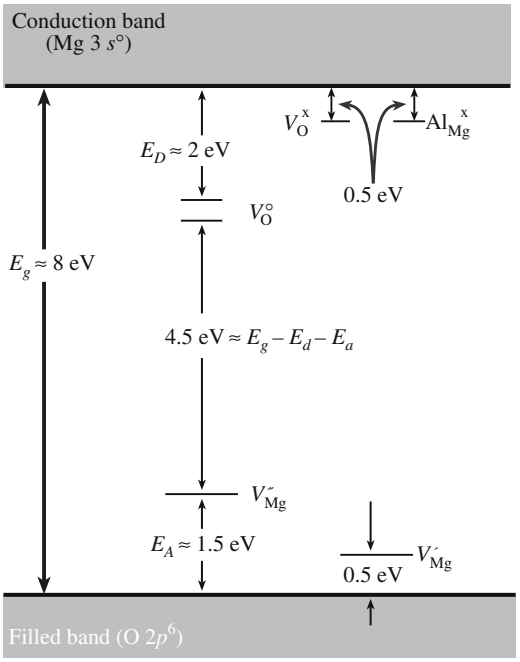

FIGURE 30.26 Defect levels in MgO.

$$\left(V_O^x\right) \rightarrow \left(V_O^{\cdot}\right) + e' \tag{30.42}$$

You will notice that Kröger–Vink notation is useful for describing this process. The energy for ionization is 0.5 eV and can be represented as a level just below the bottom of the conduction band—the oxygen vacancy is behaving as a donor.

The oxygen vacancy can become doubly ionized:

$$\left(V_O^{\cdot}\right) \rightarrow \left(V_O^{\cdot\cdot}\right) + e' \tag{30.43}$$

The energy for this second ionization process is ~2 eV and can be represented as another donor level.

In a similar way we can represent acceptor sites within the band diagram for MgO as being due to the oxidation of MgO, i.e., the introduction of magnesium vacancies and corresponding holes. The following reactions show the origin of the acceptor levels:

$$\left(V_{Mg}^x\right) \rightarrow \left(V_{Mg}'\right) + h^{\cdot} \tag{30.44}$$

and

$$\left(V_{Mg}'\right) \rightarrow \left(V_{Mg}''\right) + h^{\cdot} \tag{30.45}$$

The energies for these two processes are 0.5 eV and ~1.5 eV, respectively. Even though these ionization energies are relatively small compared to the band gap, the concentration of these defects is extremely low. Even at temperatures >2000°C the number of cation and anion vacancies in MgO is only about one per billion lattice sites.

The addition of substitutional and interstitial point defects can also introduce additional energy levels. Using MgO as our example let us consider the incorporation of Al_2O_3. There are two defect reactions we can envision:

$$Al_2O_3 \xrightarrow{MgO} 2\left(Al_{Mg}\right)^{\cdot} + \left(3O_O\right)^x + \left(V_{Mg}\right)'' \tag{30.46}$$

and

$$Al_2O_3 \xrightarrow{MgO} 2\left(Al_{Mg}\right)^{\cdot} + \left(O_O\right)^x + O_2 + 2e' \tag{30.47}$$

In Eq. 30.46 the incorporation of Al into Mg sites is compensated for by the formation of a magnesium vacancy. This type of incorporation is termed ionically compensated because an ionic defect has compensated for the charge difference. The second reaction, given by Eq. 30.47, is electronically compensated because electrons (or in some cases holes) are compensating for the charge difference resulting from the substitution of a divalent cation

for a trivalent one. Acceptor levels are introduced by ionic compensation, and electronic compensation corresponds to the introduction of donor levels in the energy gap.

CHARGE BALANCE

Reminder: Reactions expressed using Kröger–Vink notation must be charged balanced, just like regular chemical reaction equations.

Combining Eqs. 30.46 and 30.47 we can write

$$2O_2 + 2e' \leftrightarrow (2O_o)^x + (V_{Mg})'' \qquad (30.48)$$

Stoichiometric oxides such as MgO are very difficult to reduce and hence the reaction represented by Eq. 30.48 is strongly to the right throughout all accessible ranges of temperature and oxygen activity. Even highly doped compositions are not electrically conductive at room temperature. The defects with a positive effective charge are donors; these have given up an electron to become ionized positively relative to the perfect lattice site. Correspondingly, defects with a negative effect charge are acceptors, having accepted electrons relative to the perfect lattice.

Dislocations are defects that also create additional energy levels within the band gap. They act as acceptors as shown in Figure 30.27. Note that the dislocation-acceptor levels are usually in the upper half of the band gap. Dislocations are particularly deleterious to the behavior of semiconductors. One of the main factors that limited the increase in the size of silicon wafers has been the need to grow dislocation-free single crystals. At the beginning of the semiconductor industry in the 1960s wafer sizes were limited to 2-inch-diameter wafers; now 18-inch-diameter wafers are possible because of better control of the growth parameters.

To understand why dislocations act as acceptors consider the illustration of a dislocation in silicon shown in Figure 12.11. The dislocation creates dangling bonds, which act as electron traps to satisfy the requirement of each silicon atom to achieve a noble gas electron configuration.

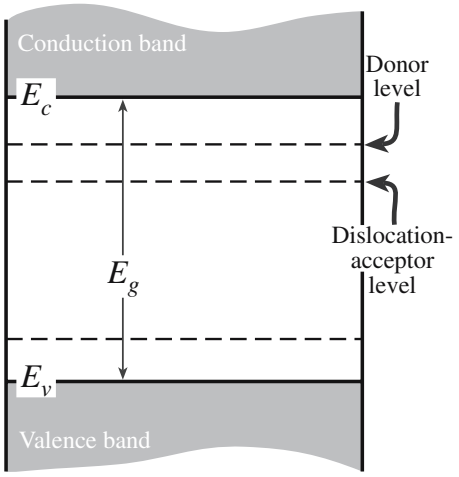

FIGURE 30.27 Effect of dislocations on the energy band diagram of a semiconductor.

Ceramics with high ρ are important for a number of applications, many of which utilize more than just the high ρ. Other properties such as high strength, stability at elevated temperature, high thermal conductivity, and hermeticity (impervious to the environment) are also important.

One application that you may be familiar with is the use of alumina ceramics as the insulator in spark plugs. The insulator must be able to withstand a peak voltage of about 10 kV at each spark discharge, a pressure pulse of about 10 MPa, and the thermal radiation from the combustion temperature that is typically 2000°C. This combination of requirements can be met only by a ceramic.

A very visible application of ceramic insulators is as power line insulators. For this application the strength of the ceramic is very important because the insulator supports a considerable weight. The insulator must also be resistant to weather damage and to absorption of water, which can lead to arcing. One ceramic used for this application is porcelain. A typical porcelain composition would lie in the following ranges: clays [e.g., kaolinite $Al_2(Si_2O_5)(OH)_4$], 40–60 wt%, flux [e.g., orthoclase ($KAlSi_3O_8$)], 15–25 wt%, and quartz or bauxite filler, 30–40 wt%. The porcelain is known as a "silicious porcelain" if quartz is used as the filler and an "aluminous porcelain" if bauxite is used.

The above applications are visible uses for ceramic insulators. The two applications that we are going to emphasize next may not be ones that immediately come to mind when you think of ceramic insulators, but they are extremely important and, in fact, the development of personal computers and other electronic devices owes much to the use of insulating ceramics.

30.18 SUBSTRATES AND PACKAGES FOR INTEGRATED CIRCUITS

Substrates and packages for integrated circuits (ICs) constitute the largest application for ceramic insulators. The following properties are required:

- High ρ
- High thermal conduction
- Low dielectric constant
- Hermetic

Three ceramics are usually used for this application:

- Al_2O_3
- BeO
- AlN

Alumina ceramics dominate, but there are important reasons why BeO and AlN are used in certain applications. Table 30.11 compares the properties of these three

TABLE 30.11 Physical Properties of Substrate Materials

Property	*96%Al_2O_3*	*99.5% Al_2O_3*	*BeO*	*AlN*	*Mullite*	*Glass-ceramics*
Density (g/cm^3)	3.75	3.90	2.85	3.25	2.82	2.5–2.8
Flexural strength (MPa)	400	552	207	345	186	138
Thermal expansion from 25 to 500°C (ppm/°C)	7.4	7.5	7.5	4.4	3.7	3.0–4.5
Thermal conductivity at 20°C ($W m^{-1}°C^{-1}$)	26	35	260	140–220	4	4–5
Dielectric constant at 1 MHz	9.5	9.9	6.7	8.8	5.4	4–8
Dielectric loss at 1 MHz (tan δ)	0.0004	0.0002	0.0003	0.001–0.0002	0.003	>0.002

ceramics and some others that have also been used as substrates and packages. BeO and AlN are used in situations in which high thermal conductivity is needed. Heat removal from power electronics and from integrated circuits is determined mainly through the substrate; one factor that influences the heat transfer rate is the thermal conductivity of the substrate material. Effective thermal management is important in improving the reliability of electronic devices.

AlN has a theoretical thermal conductivity of 320 $W m^{-1} K^{-1}$ and values as high as 285 $W m^{-1} K^{-1}$ have been experimentally measured for single crystals. Commercial AlN substrates are available with a thermal conductivity up to about 200 $W m^{-1} K^{-1}$ at room temperature. The thermal expansion of AlN ($3.9 \times 10^{-6} K^{-1}$) from room temperature to 500 K is very similar to that of silicon ($3 \times 10^{-6} K^{-1}$) over the same temperature interval, which helps to avoid cracking due to thermal misfit stresses between substrate and device. This consideration is particularly important for large silicon chips. AlN also does not have the inherent toxicity problems associated with BeO.

30.19 INSULATING LAYERS IN INTEGRATED CIRCUITS

Layers of SiO_2 have several uses in the production of silicon ICs:

- Device isolation
- Isolation of multilevel metallization
- Surface passivation
- The gate oxide in metal–oxide–semiconductor (MOS) structures
- Barrier layer during dopant incorporation.

SiO_2 layers can be obtained by direct oxidation by one of the following reactions:
Dry oxidation:

$$Si\ (s) + O_2\ (g) \rightarrow SiO_2\ (s) \qquad (30.49)$$

Wet oxidation:

$$Si\ (s) + 2H_2O\ (g) \rightarrow SiO_2\ (s) + 2H_2\ (g) \qquad (30.50)$$

Dry oxidation is slow, but produces a uniform relatively defect-free layer that is electrically very reliable. Wet oxidation is more frequently used for masking operations because the growth rate is faster, however, the layers are not as uniform as those produced by dry oxidation.

The oxide layer formed on the silicon surface is what is known as a protective oxide. The growth rate initially follows a linear rate law, i.e., the oxide thickness, x, increases linearly with time, t

$$x \propto t \qquad (30.51)$$

For the two processes the activation energies are

$E_A = 1.96$ eV for wet oxidation
$E_A = 2.0$ eV for dry oxidation

These values are close to the energy required to break the Si–Si bond, 1.83 eV.

After a layer of approximately 100 nm has formed the growth kinetics follow a parabolic rate law, i.e., the oxide thickness increases with the square root of time:

$$x \propto \sqrt{t} \qquad (30.52)$$

Diffusion through the oxide layer follows an Arrhenius law (Eq. 3.13):

$E_A = 1.24$ eV for dry oxidation
$E_A = 0.71$ eV for wet oxidation

These activation energies are close to those for the diffusivity of oxygen and water vapor through fused silica, respectively. Fused silica has a structure very similar to that of thermal SiO_2.

When very thin SiO_2 layers are required such as a gate oxide in an MOS-field effect transistor (MOSFET) or when an SiO_2 layer is required as an insulating layer between layers in a multilevel device the CVD process is used. The dielectric is an active component of the storage capacitor in dynamic RAMs, and its thickness determines the amount of charge that can be stored (see Chapter 31).

In a complementary metal-oxide semiconductor (CMOS) device oxidation of polysilicon is necessary for electrical isolation. A thermal oxide can be produced on polysilicon in a manner similar to that produced on single crystal silicon.

30.20 SUPERCONDUCTIVITY

There are two properties that a material must possess to be considered a superconductor:

1. $\rho = 0$
2. $B = 0$ (described in Chapter 33)

Zero resistivity is observed in a superconductor at all temperatures below a critical temperature, T_c, as illustrated in Figure 30.28. At T_c the material changes from a state of normal conduction to the superconducting state. In the superconducting state an induced current will flow indefinitely: without loss. This behavior has been demonstrated experimentally when a current has been run through a closed ring of a superconducting metal for over two and a half years without any measurable decay.

Superconductivity has been observed in *all* the classes of materials: metals, ceramics, and polymers. Of all the elements in the periodic table only 27 are known to become superconducting under ordinary pressure. Niobium is the element with the highest T_c, 9.2 K, whereas for tungsten T_c is only 0.0154 K. An interesting fact is that metals having the highest σ, e.g., Cu, Ag, and Au, are not superconducting even at extremely low temperatures, if at all. It is the metals that are the poorer electrical conductors that make

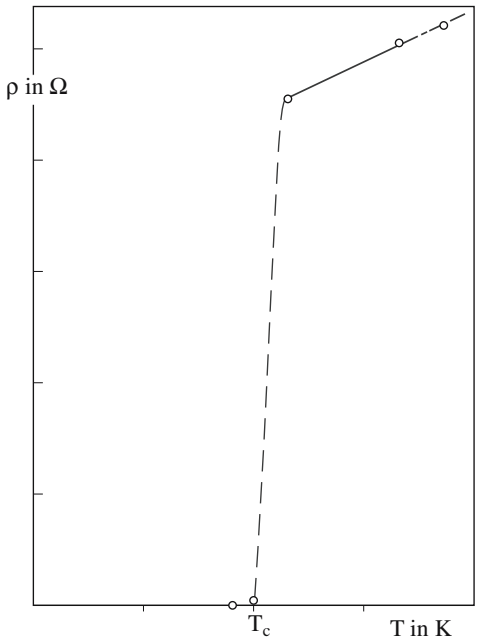

FIGURE 30.28 Plot of ρ versus T for a superconductor.

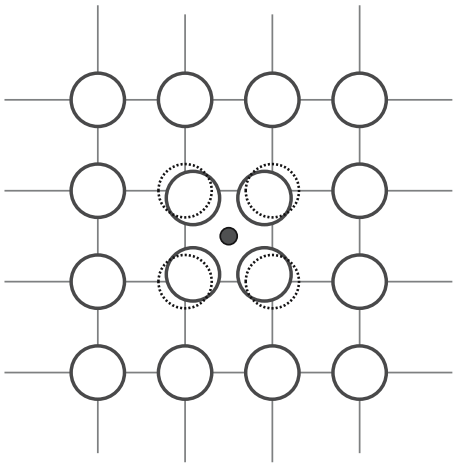

FIGURE 30.29 Illustration of lattice distortion around a free electron, which leads to the formation of Cooper pairs.

the better superconductors, albeit still at very low temperatures. Low-temperature superconductors (LTSC) have a T_c up to about 20 K. High-temperature superconductors (HTSC) are usually defined as having a T_c above the boiling temperature of liquid nitrogen.

The BCS theory (after Bardeen, Cooper, and Schrieffer) provides an explanation for superconductivity at low temperatures. The theory is complicated, but the basis is that there exists an attractive force between electrons that have about the same energy. This force causes them, under the right circumstances, to move in pairs. These are the so-called Cooper pairs. The criterion for superconductivity is that this attraction should be greater than the natural repulsion between like charges. T_c corresponds to the binding energy needed to hold the Cooper pairs together in a superconducting state.

The origin of the attractive force is that in a lattice of positive ions, an electron will attract the positive ions toward itself. In this region the lattice will be slightly denser as shown in Figure 30.29. To a passing electron the local lattice distortion will appear as an increase in positive charge density and it will be attracted toward it. The two electrons pair up in this way through their interaction with the lattice.

If the lattice is vibrating through thermal effects pairing will not be possible, but at very low temperatures where the vibration amplitude is small, the attractive force can be dominant. The electrons are held together by a binding energy of only about 10^{-4} eV. The separation of the electrons in the pair (called the coherence length) for most LTSC is 100 nm. Interatomic spacings are on the order of 0.3 nm, so two bound electrons can be as far apart as 300 lattice spaces. The large coherence length means that defects such as dislocations, GBs, and impurities are too small to have much effect on superconducting behavior.

The existence of these bound electron pairs alters the energy band diagram for a superconductor by introducing

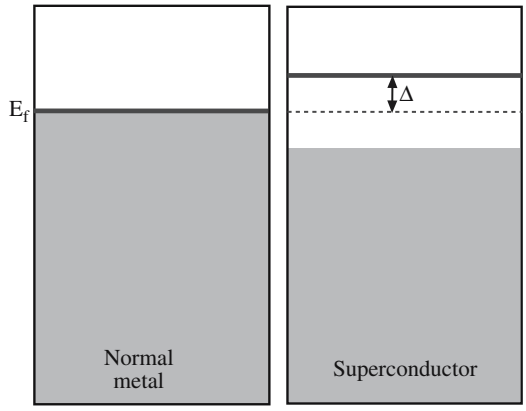

FIGURE 30.30 Band diagram for a superconductor.

a small gap at E_F, known as the superconducting gap, Δ. The difference in the band structure of a material in the superconducting state and in the nonsuperconducting state is illustrated in Figure 30.30. The energy of this gap corresponds to the binding energy of the electron pairs. An energy 2Δ is needed to break a Cooper pair. The relationship between Δ and T_c is given by the BCS theory:

$$2\Delta = 3.5\,kT_c \qquad (30.53)$$

- For LTSC Δ ~1 meV
- For HTSC Δ ~1–10 meV

The BCS theory predicts an ultimate limiting value of T_c of 30 K for electron pairing via lattice vibrations (phonons). This limit was enough to stop many researchers from pursuing careers in superconductivity. But clearly the BCS theory, in its entirety, cannot be applicable to HTSC where $T_c \gg 30$ K. In these materials pairing of the electrons still occurs, but the mechanism that allows this pairing needs to be determined.

CHEVREL PHASES

These are complex forms of MoS_2 having the general formula $M_xMo_6X_8$, where M is a metal and X is a chalcogen. $PbMo_6S_8$ has the highest T_c of the Chevral phases ($T_c = 15$ K). They are named after French scientist Roger Chevrel.

30.21 CERAMIC SUPERCONDUCTORS

The earliest nonmetallic superconductors were NbO and NbN. Both materials have a rocksalt crystal structure. What was significant about the discovery of superconductivity in these materials (they are of no practical use) is that they linked the phenomenon to ceramics and cubic crystal structures.

Superconductivity in a multicomponent oxide was first observed in $SrTiO_3$. Although T_c was determined to be only 0.3 K, $SrTiO_3$ has the very important perovskite structure, which, as shown in Chapter 7, is the structural building block of all presently known HTSC.

The beginning of HTSC started in 1986 with the discovery of superconductivity in the compound La_2BaCuO_4, which has T_c ~38 K. This discovery was of monumental importance because the classic BCS theory for superconductivity predicted a maximum value of T_c of only 30 K! Many more HTSC were simply obtained by systematic substitution of elements into the basic perovskite unit. Certainly in the early days many scientists said that research in HTSC was more akin to cooking than any area of science!

The elements yttrium and lanthanum are interchangeable in terms of chemical properties (they are in the same group in the periodic table) although they differ in size. The same is true of strontium and barium in Group II of the periodic table. The idea behind the substitution of the large element for a smaller element was based on observations that T_c could be raised under an applied pressure. Substitution of a larger element for a smaller one was thought to produce an internalized pressure effect. Table 30.12 lists some of these compounds and their T_c.

Tables 30.13 compares properties of HTSC and LTSC; v_F is the velocity of propagation of conduction electrons through crystal.

TABLE 30.12 Critical Temperatures of Some Ceramic Superconductors

Compound	T_c *(K)*
$La_{2-x}M_xCuO_{4-y}$ M = Ba, Sr, Ca $x \sim 0.15$, y small	38
$Nd_{2-x}Ce_xCuO_{4-y}$ (electron doped)	30
$Ba_{1-x}K_xBiO_3$ (isotropic, cubic)	30
$Pb_2Sr_2Y_{1-x}Ca_xCu_3O_8$	70
$R_1Ba_2Cu_{2+m}O_{6+m}$ R: Y, La, Nd, Sm, Eu, Ho, Er, Tm, Lu	
$m = 1$ (123)	92
$m = 1.5$ (247)	95
$m = 2$ (124)	82
$Bi_2Sr_2Ca_{n-1}Cu_nO_{2n+4}$	
$n = 1$ (2201)	~10
$n = 2$ (2212)	85
$n = 3$ (2223)	110
$Tl_2Ba_2Ca_{n-1}Cu_nO_{2n+4}$	
$n = 1$ (2201)	85
$n = 2$ (2212)	105
$n = 3$ (2223)	125

TABLE 30.13 Comparison of Superconductors in the Normal State

Material	Number of conduction electrons (n) (electrons/cm^3)	Fermi velocity (v_F) (m/s)	Mean free path (λ_e) (nm)	ρ (@ 100 K) ($\mu\Omega\cdot$cm)	χ (nm)
Al	180×10^{21}	2.0×10^6	130	0.3	1600
Nb	56×10^{21}	1.4×10^6	29	3	38
LSCO	5×10^{21}	0.1×10^6	~5	~100	~1.5
YBCO	7×10^{21}	0.1×10^6	~10	~60	~1.0

- The obvious difference is T_c. The fact that $T_c \sim 10^2$ K means that the binding energy is ~10 meV, as compared to <1 meV in LTSC.
- The ceramics have higher ρ than the metals at 100 K. But ρ is comparable to some of the best ceramic electrical conductors, such as CrO_2 and TiO.
- For HTSC χ is only ~1.0 nm, which means that the pairing behavior is almost on an atomic scale and the superconducting properties will be dependent on atomic scale defects. (Compare χ with the width of a dislocation or GB.) Such defects therefore scatter the electron pairs and reduce the critical current density. For metals χ is large, e.g., $\chi = 1.6\,\mu$m in pure Al, $\chi =$ 38 nm in pure Nb.
- χ is anisotropic. For YBCO $\chi_{ab} \sim 1.5$ nm and $\chi_c \sim$ 0.4 nm. A major problem in HTSC is to find a crystal defect that pins the flux vortices, but does not disrupt current flow.

We showed the structures of HTSC in Chapter 7. Superconductivity essentially takes place within the CuO_2 planes. The Cu–O chains can be considered as a "charge-reservoir" that is needed to transfer charge into the CuO_2 planes. Charge carriers are added by doping: adding oxygen to $YBa_2Cu_3O_6$, which enters the compound as O^{2-} and forms Cu–O chains. To maintain charge balance, electrons are removed from the Cu–O planes and the remaining holes are mobile (hence conduction) and form Cooper pairs below T_c.

In LTSC Cooper pairs, with a charge of –2e, are responsible for current flow. In most of the HTSC the Cooper pairs have a positive charge, +2e. In other words they are positive holes and the charge transfer process can be written as

$$Cu^{2+} + h^+ \rightarrow Cu^{3+} \qquad (30.54)$$

One of the consequences of a hole-hopping process involving a two-dimensional array of copper ions is that the superconducting current is very anisotropic. Hopping tends to occur between copper ions that have the smallest separation from each other, namely those in the plane. The distance between copper ions on adjacent planes is much larger than within the planes; hence charge hopping between planes is much less efficient.

There are many potential applications for HTSC, but the actual realization of these has in many cases not occurred. The major problem is being able to fabricate the ceramics into useful and usable shapes. Ceramics are inherently brittle and this alone makes the fabrication of long wires and tapes extremely difficult. These would be essential for domestic and industrial power transmission (some limited progress has been made in this area as we describe in Chapter 37). The low χ also makes practical applications more difficult to achieve because we have to be concerned about defects.

The most likely route to widespread practical application is to use the HTSC in the form of a thin film and utilize the Josephson effect. The original observation of this effect was made using a junction consisting of two superconductors separated by a very thin insulating layer (~1 nm). In thin films the "insulating" region can be orientation changes across a GB as shown in Figure 14.37.

The *I–V* characteristics of a Josephson junction are very nonlinear as shown in Figure 30.31. The key features are as follows:

- When $V = 0$, a direct current flows.
- When a small voltage is applied $I = 0$.
- At V_c the electrons are no longer paired and normal electron tunneling occurs with associated resistive losses.

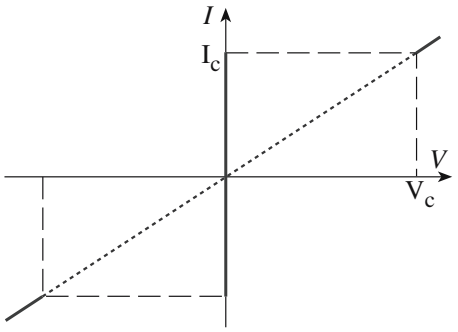

FIGURE 30.31 *I–V* characteristics of a Josephson junction.

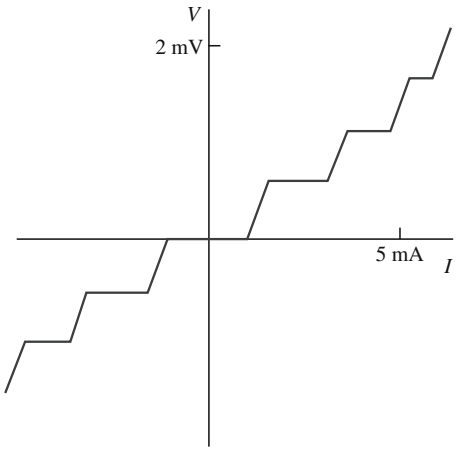

FIGURE 30.32 Effect of incident microwave radiation on the *I–V* characteristics of a Josephson junction.

If a Josephson junction is irradiated with microwaves of frequency *f*, the *I–V* behavior shows a series of steps, called Shapiro steps, as shown in Figure 30.32. These steps correspond to supercurrents across the junction when the condition for the absorption of microwave photons is satisfied (this is called the ac Josephson effect). Similar behavior is seen when we expose the junction to a magnetic field. How Josephson junctions can be used to detect very small magnetic fields is described in Chapter 33.

CHAPTER SUMMARY

We can explain the wide range of electrical properties shown by ceramics by considering their electron band structure. Some oxides show metallic-like levels of conductivity consistent with either a partially filled valence band or a small E_g. These materials are used as electrodes and conductors. Most ceramics fall into the category of having a medium to wide E_g. Semiconducting ceramics are used in a variety of sensors. The most important application is to "sense" anomalous voltages. As with the more familiar Si and GaAs, which are also ceramics, the conductivity of all semiconductors can be changed by doping. Unlike Si and GaAs we can use stoichiometry changes to modify σ. Ceramics having the largest E_g usually show a significant degree of ionic bonding and any conductivity is mainly associated with ion transport. The important technological example is cubic ZrO_2, which is the electrolyte in solid oxide fuel cells. Fuel cells are one of the key components of a "hydrogen economy." We finished this chapter with superconductors. The structure of these materials is already familiar from Chapter 7 and the importance of GBs as weak links from Chapter 14.

PEOPLE IN HISTORY

Bardeen, John (1908–1991) received the 1972 Nobel Prize in physics with Cooper and Schrieffer for the BCS theory. It was his second Nobel Prize! He won his first in 1956 for his role in the invention of the transistor.

Cooper, Leon Neil (1930–) received the Nobel Prize in physics with Bardeen and Schrieffer for the BCS theory. Cooper pairs are named after him.

Drude, Paul Karl Ludwig (1863–1906) was a German physicist who developed a theory for electron conduction. Drude's theory provided an atomistic basis for understanding electron motion in metals and ceramics. In its original version it contained several inaccuracies, which were corrected by the application of quantum mechanics.

Grove, Sir William Robert (1811–1896) was a British scientist who in 1839 discovered the principle on which fuel cells are based. His cell, which was composed of two Pt electrodes both half immersed in dilute H_2SO_4, one electrode fed with O_2 and the other with H_2, was not a practical method for energy production.

Onnes, Heike Kamerlingh (1853–1926) was a Dutch physicist who succeeded in liquefying helium in 1908 and discovered superconductivity in mercury in 1911. He wrote at the time: *Mercury has passed into a new state, which on account of its extraordinary electrical properties may be called the superconducting state*. He received the Nobel Prize in physics in 1913.

Schrieffer, John Robert (1931–) received the Nobel Prize in physics with Bardeen and Cooper for the BCS theory.

GENERAL REFERENCES

Cox, P.A. (1987) *The Electronic Structure and Chemistry of Solids*, Oxford University Press, Oxford. A very good description of electronic properties.

Cyrot, M. and Pavuna, D. (1992) *Introduction to Superconductivity and High-Tc Materials*, World Scientific, Singapore. A clear introduction to the field. Treats the theoretical models at a level above that used here but within the range of most upper division MSE undergraduates and graduate students.

Duffy, J.A. (1990) *Bonding, Energy Levels and Bands in Inorganic Solids*, Longman Scientific and Technical, Harlow, Essex, UK. Straightforward description of energy bands in solids.

Hench, L.L. and West, J.K. (1990) *Principles of Electronic Ceramics*, Wiley, New York. Comprehensive background to electronic ceramics.

Moulson, A.J. and Herbert, J.M. (1992) *Electroceramics*, Chapman & Hall, London. An excellent account of the properties and applications of electroceramics.

Owens, F.J. and Poole, C.P. Jr. (1996) *The New Superconductors*, Plenum Press, New York.

SPECIFIC REFERENCES

Bardeen, J., Cooper, L.N., and Schrieffer, J.R. (1957) "Theory of superconductivity," *Phys. Rev.* **108**, 1175. The BCS theory in all its technical detail.

Josephson, B.D. (1962) "Possible new effects in superconductive tunneling," *Phys. Lett.* **1**, 251. The eponymous junction.

Nye, J.F. (1985) *Physical Properties of Crystals*, Clarendon Press, Oxford. This is the standard reference for tensor representation. Chapter XI covers transport properties including electrical conductivity. The representation of σ by tensors is not necessary to understand the electrical behavior of materials. Its significance becomes clear when we want to specify certain properties of anisotropic single crystals.

JOURNALS

Solid State Ionics. An international journal published by Elsevier.

Journal of Electronic Materials. Published by ASM.

Journal of Materials Science: Materials in Electronics. Published by Springer.

JOURNALS DEVOTED TO SUPERCONDUCTIVITY AND ITS APPLICATIONS

The field of high-temperature superconductivity experienced unprecedented growth during the late 1970s and 1980s. The important aspects of much of that research have been compiled in several books. Even so the field is still producing new developments, although of a much more incremental nature, and journals are the best place to find out what is happening. The following journals deal exclusively with superconductivity.

Physica C. Published by Elsevier.

Journal of Superconductivity since January 2006 renamed the *Journal of Superconductivity and Novel Magnetism*. Published by Springer.

Superconductor Science and Technology. Published by the Institute of Physics (IOP).

OTHER JOURNALS REPORTING DEVELOPMENTS IN HTSC

Many other journals have regular contributions in the area of HTSC. The major resources are listed below.

Journal of Applied Physics. Published by the American Institute of Physics (AIP).

Applied Physics Letters. Also published by AIP. Consists of three page papers covering important developments in applied physics. A repository for many of the early papers covering processing of HTSC films.

Physical Review B, Physical Review Letters, Japanese Journal of Applied Physics, *Journal of Materials Science: Materials in Electronics.*

EXERCISES

30.1 Using Table 30.2 explain the following: (a) Why do t_+ and t_- change for NaCl as the temperature is increased from 400 to 600°C. (b) How would you expect these numbers to change if the temperature was increased further to 700°C? (c) Why is t_e zero?

30.2 At what temperature would the probability of finding an electron in the conduction band of diamond be the same as the probability of finding an electron in the conduction band of silicon at 25°C?

30.3 Using appropriate sketches compare the ion arrangements in the electrical conductor TiO shown in Figure 30.5 to those in the electrical insulator MgO.

30.4 In glasses containing alkali metal oxides such as Na_2O, the current is carried almost entirely by the alkali metal ion. (a). What is the transference number for alkali metal ions in this case? (b) Sketch the potential energy barrier for ion transport (i.e., redraw Figure 30.20 for a glass). (c) Why does your figure look different from Figure 30.20?

30.5 Calculate the probability of an electron being in the conduction band of MgO at a temperature of 2000°C.

30.6 The Hope diamond exhibited at the Smithsonian Institution in Washington, D.C. is a striking blue. Would you expect this stone to be electrically conducting? Explain how you arrived at your answer. Make sure to mention any assumptions you make.

30.7 What is the HTSC that currently has the highest T_c? Are there any practical problems related to the use of this material?

30.8 In ZrO_2 (fluorite structure) ion conduction is the result of anion motion. In Li_2O (antifluorite structure) would you consider the anions or cations to be more mobile? (b). How might you increase ion conductivity in Li_2O? In both cases explain how you arrived at your answer. (c) Now repeat (a) and (b) for MgO.

30.9 GaN is a wide-band-gap semiconductor. (a) What is E_g for GaN? (b) Describe some possible applications for GaN.

30.10 Dislocations have been shown to decrease the mobility of electrons in a semiconductor. Using the illustration of a dislocation in Figure 12.11 explain why you think they have a detrimental effect on μ.